Connecting thermal physiology and latitudinal niche partitioning in marine Synechococcus

Justine Pittera, Florian Humily, Maxine Thorel, Daphné Grulois, Laurence Garczarek, Christophe Six

Connecting thermal physiology and latitudinal niche partitioning in marine *Synechococcus*

Pittera Justine[1,2], Humily Florian[1,2], Thorel Maxine[3], Grulois Daphné[1,2], Garczarek Laurence[1,2] & Christophe Six[1,2]

[1] University Pierre and Marie Curie (Paris 06), UMR 7144, Marine Phototrophic Procaryotes (MaPP) Team, Station Biologique de Roscoff, Place Georges Teissier, CS 90074, 29688 Roscoff cedex, France.

[2] Centre National de la Recherche Scientifique, UMR 7144, Oceanic Plankton Group, Station Biologique de Roscoff, Place Georges Teissier, CS 90074, 29688 Roscoff cedex, France.

[3] University of Caen-Basse Normandie et Centre National de la Recherche Scientifique, Institut d'Ecologie et d'Environnement, FRE 3484 Biologie des Mollusques Marins et des Ecosystèmes associés, 14032 Caen, France.

Running title: Temperature adaptation in marine *Synechococcus*

To whom correspondence should be addressed: Christophe Six, christophe.six@sb-roscoff.fr

Submitted to: the ISME Journal

Abstract

Marine *Synechococcus* cyanobacteria constitute a monophyletic group that displays a wide latitudinal distribution, ranging from the equator to the polar fronts. Whether these organisms are all physiologically adapted to stand a large temperature gradient or stenotherms with narrow growth temperature ranges has so far remained unexplored. We submitted a panel of six strains, isolated along a gradient of latitude in the North Atlantic Ocean, to long- and short-term variations of temperature. Upon a downward shift of temperature, the strains showed strikingly distinct resistance, seemingly related to their latitude of isolation. This behaviour was associated to differential photosynthetic performances, with tropical strains collapsing while northern strains were capable of growing. In the tropical strains, the rapid photosystem II inactivation and the decrease of the antioxydant β-carotene relative to chl *a* suggested a strong induction of oxidative stress. These different responses were related to the thermal *preferenda* of the strains. The northern strains could grow at 10°C whilst the other strains preferred higher temperatures. In addition, we pointed out a correspondence between strain isolation temperatures and phylogeny. In particular, clade I and IV laboratory strains were all collected in the coldest waters of the distribution area of marine *Synechococus*. We however show that clade I *Synechococcus* exhibit different levels of adaptation, which apparently reflect their location on the latitudinal temperature gradient. This study reveals the existence of lineages of marine *Synechococcus* physiologically specialised in different thermal niches, therefore suggesting the existence of temperature ecotypes within the marine *Synechococcus* radiation.

Keywords: Adaptation / Ecotype / Marine cyanobacteria / *Synechococcus* / Temperature

Subject category: Microbial ecology and functional diversity of natural habitats

Introduction

Marine picocyanobacteria belonging to the *Prochlorococcus* and *Synechococcus* genera are major contributors to carbon biomass and global oceanic primary production and may contribute up to half of the fixed carbon in some oceanic regions (Li 1994, Liu *et al.* 1997, Buitenhuis *et al.* 2012). Although phylogenetically closely related, these two cyanobacteria exhibit distinct traits of ecology, physiology and evolution (Partensky *et al.* 1999, Partensky and Garczarek 2010). While *Prochlorococcus* thrives in warm waters of the latitudinal 45°N-40°S band, *Synechococcus* cells prefer coastal and mesotrophic open ocean waters, with a much wider latitudinal distribution ranging from the equator to the polar fronts (Not *et al.* 2005, Zwirglmaier *et al.* 2008, Huang *et al.* 2011). In addition, *Synechococcus* has no obvious depth preference, the highest cell densities being often observed in the upper mixed layer, whereas *Prochlorococcus* shows strong depth partitioning, with two main ecotypes that are both physiologically and genetically distinct: a high light-adapted (HL) ecotype, occupying the upper part of the euphotic zone and a low light-adapted ecotype (LL), dominating the bottom of the euphotic layer (Moore *et al.* 1998). More recently, the HL ecotype has been further subdivided into HLI and HLII, which exhibit distinct latitudinal distributions, HLII dominating between 28°S to 33°N and HLI above 32°S or 38°N, a difference seemingly linked to the different temperature growth optima of their cultured representatives (Johnson *et al.* 2006, Zinser *et al.* 2007).

Using the 16S rRNA and ITS genetic markers, respectively ten and fifteen different clades (Rocap *et al.* 2002, Fuller *et al.* 2003) have been delineated within the main group of the marine *Synechococcus* radiation (cluster 5.1; *sensu* Herdman *et al.* 2001). However, a recent study by Mazard and colleagues (2012a) has highlighted a greater genetic microdiversity than previously thought in this subcluster. Indeed, using the cytochrome b_6 gene *petB*, they could define more than thirty different subclades of marine *Synechococcus.*

Because of this large number of lineages, the environmental factors that have directed the diversification of marine *Synechococcus* appear much more complicated to understand than in the case of *Prochlorococcus*. Through a vast phylogeographic study, Zwirglmaier and co-workers (2007, 2008) have however shown that, out of the dozen of marine *Synechococcus* 16S rRNA clades, only four (I to IV) predominate in the oceans. While clades I and IV generally co-occur at latitudes above 30°N/S and at depth, clade II seems to prevail in warm, coastal or shelf areas (Zwirglmaier *et al.* 2007, 2008, Huang *et al.* 2011, Mella-Flores *et al.* 2011, Ahlgren and Rocap 2012). The latitudinal distribution of clade III appears to be broader, but with an apparent predominance in oligotrophic, offshore waters (Fuller *et al.* 2005, Zwirglmaier *et al.* 2008, Mella-Flores *et al.* 2011, Post *et al.* 2011). The other clades are usually detected at low concentrations and their distribution patterns are less clearly defined (Zwirglmaier *et al.* 2008, Huang *et al.* 2011).

To understand whether some *Synechococcus* lineages are adapted to specific ecological niches, both phylogeography and comparative physiology studies are necessary. These two approaches indeed allow pointing out possible correspondences between cell performances, phylogeny and ecological niches. So far, most of the comparative studies of marine *Synechococcus* physiology have dealt with adaptation and acclimation capacities to light (Six *et al.* 2004, 2007b, 2007c) and nutrients variations (e.g. Liu *et al.* 2012, Mazard *et al.* 2012b). These works suggest that marine *Synechococcus* strains can grow over large ranges of irradiance, explaining that cells of this organism are detected from surface down to 150 m (Kana and Glibert 1987, Olson *et al.* 1990, Moore *et al.* 1995, Six *et al.* 2004, 2007b). Light quality also influences marine *Synechococcus* distribution (Olson *et al.* 1990, Lantoine and Neveux 1997, Wood *et al.* 1998, Sherry and Wood 2001). The pigmentation of the light-harvesting complex, the phycobilisome (PBS), is indeed highly variable among strains (Six *et al.* 2007b, 2007c, 2009) and optimized to collect the most abundant wavelengths in a given

light niche. These different pigment types, however, most often are not restricted to specific *Synechococcus* lineages (Palenik 2001, Six *et al.* 2007c), and therefore do not constitute ecotypes *sensu stricto*. Similarly, although nutrient availability contribute to some of the variability of the *Synechococcus* community structure (Zwirglmaier *et al.* 2008, Mazard *et al.* 2012a), a clear delineation of nutrient ecotypes (equivalent to *Prochlorococcus* light ecotypes) within the *Synechococcus* radiation remains globally elusive (Palenik *et al.* 2006, Scanlan *et al.* 2009, Stuart *et al.* 2009). A notable exception concerns the response to phosphorus limitation (including cell size change and the ability to accumulate polyphosphate) that appears somewhat consistent with *Synechococcus* phylogeny and their inferred ecology of the different clades (Mazard *et al.* 2012a). However, a large part of the variation observed in the *Synechococcus* community structure and the hierarchy of environmental factors shaping ecotype genomes remains largely unexplained.

Adaptation to temperature variations among marine *Synechococcus* has been so far poorly explored. This environmental factor can significantly constrain growth, as the activity of most enzymes and biomembranes directly depends on it, thus impacting major metabolic processes. Among them, photosynthesis is known to be particularly affected by temperature variations, notably because of the resulting changes in thylakoidal fluidity that eventually lead to photosystem (PS) II inactivation (Murata and Los 1997, Takahashi and Murata 2008). Like for *Prochlorococcus* (Johnson *et al.* 2006, Zinser *et al.* 2007), temperature might have thus played an important role in the differentiation of the *Synechococcus* lineages, possibly influencing significantly their genome shaping. However, given the scarcity of physiological studies of the response of open ocean *Synechococcus* isolates to temperature (Moore *et al.* 1995, Fu *et al.* 2007), it is difficult to assert whether the large latitudinal distribution of these picocyanobacteria is rather the result of broad acclimation capacities to temperature, or of

adaptation processes underlying the existence of different 'thermotypes' that would display distinct temperature optima for growth.

To explore these questions, we describe in this paper the short and long-term responses to temperature of a panel of six *Synechococcus* strains, isolated at various latitudes, in mesotrophic waters of the North Atlantic Ocean. We aimed at pointing out different resistance and acclimation capacities among the strains, with a focus on their capability to tune light utilisation in response to temperature variations. We furthermore highlight ecophylogenetic features of marine *Synechococcus* and discuss the importance of temperature in the diversification of this radiation.

Material and Methods

Growth conditions and experimental design

In order to minimize the differences regarding other physico-chemical parameters than temperature among isolation sites, we selected six marine phycoerythrobilin-rich (pigment type 3a , Six *et al.* 2007c; Humily et *al.* in press) *Synechococcus* strains that were isolated in the North Atlantic Ocean, at similar distance from both the West or East coast, but at very different latitudes, from the polar circles to intertropical zone (Fig. 1). Clonal *Synechococcus* spp. strains A15-37, M16.1, WH7803, ROS8604, MVIR-16-2 and MVIR-18-1 were retrieved from the Roscoff culture collection (Table 1; http://www.sb-roscoff.fr/Phyto/RCC/; Vaulot *et al.* 2004) and grown in polystyrene flasks (Nalgene, Rochester, NY, USA; or Sarsted, Nümbrecht, Germany) in PCR-S11 culture medium (Rippka *et al.* 2000) supplemented with 1 mM sodium nitrate. The seawater was reconstituted using Red Sea Salt (Houston, Texas, USA) and distilled water. Continuous white light was provided by fluorescent tubes (Sylvania Daylight F18W/54-765 T8) at 80 µmol photons m^{-2} s^{-1} irradiance. Cultures of the six strains were long-term acclimated to a range of temperatures,

from 10°C to 35°C, within temperature-controlled chambers (Liebherr-Hausgeräte, Lienz, Austria) in order to measure growth rates as a function of temperature.

For cold stress experiments, early exponentially growing cultures (1.5 L) of the six *Synechococcus* strains grown at 22 ± 1°C were transferred to 13 ± 1°C under 80 µmol photons m^{-2} s^{-1} of continuous white light. This temperature amplitude was chosen to be large enough to observe physiological readjustments in the cold resistant strains, while not causing too abrupt culture collapsing of the sensitive ones. After the transfer, about five hours were necessary for the cultures to reach 13°C. The cultures were daily sampled for cell counting, fluorescence measurements and pigment analyses as described below. These experiments were repeated at least four times and compared to control cultures, *i.e.* grown routinely at 22°C. Following the cold period of six days, cultures were shifted back to 22°C, in order to estimate their recovery capacities.

Flow cytometry

For cell density measurements, aliquots of cultures were preserved within 0.25% glutaraldehyde grade II (Sigma) and stored at -80°C until analysis (Marie *et al.* 1999). Cell concentrations were determined using a flow cytometer (FACSCanto II, Becton Dickinson, San Jose, CA, USA) for which laser emission was set at 488 nm and using distilled water as sheath fluid. For steady state acclimated cultures, growth rates (µ, in day^{-1}) were computed as the slope of a Ln(N*t*) *vs*. time plot, where N*t* is the cell concentration at time *t*. Orange and red fluorescence levels (emission at 585 ± 21 nm) were normalised with standard 0.95 µm YG beads (Polysciences Warrington, PA, USA) after analysing list mode files with the custom-designed freeware CYTOWIN (Vaulot 1989) or the FCS Express 4 Flow Research Edition software (De Novo Software, Los Angeles, CA, USA).

In vivo *fluorescence measurements*

PSII quantum yield (F_V/F_M) and non photochemical quenching associated to state transition (NPQ_{ST}) were measured upon excitation at 520 nm using a Pulse Amplitude Modulation fluorometer (Phyto-PAM, Walz, Effeltrich, Germany) equipped with a temperature controlled cuvette holder and connected to a chart recorder (Vernier, LabPro, Beaverton, OR, USA). After 5 min acclimation to dark, the maximal fluorescence levels were measured in the dark (F_{Md}) and under bright red light (655 nm, 2000 µmol photons m^{-2} s^{-1}; F_M) in the presence of 100 µM of the PSII blocker 3-(3,4-dichlorophenyl)-1,1-dimethylurea (DCMU), by triggering saturating light pulses (655 nm; 5000 µmol photons m^{-2} s^{-1}). The PSII quantum yield was calculated as:

$$F_V/F_M = (F_M-F_0)/F_M$$

where F_0 is the basal fluorescence level and F_V is the variable fluorescence (Campbell *et al.* 1998, Six *et al.* 2007a, 2009). The NPQ_{ST} factor was calculated as:

$$NPQ_{ST} = (F_M-F_{Md})/F_M$$

In addition, fluorescence emission spectra were recorded at experimental temperature (22°C or 13°C) upon excitation at 530 nm, with a LS-50B spectrofluorometer (Perkin-Elmer, Waltham, MA, USA), as described by Six *et al.* (2004, 2007b). In order to study the phycobiliprotein coupling in the PBS during the cold period, the phycoerythrin (PE) to phycocyanin (PC) fluorescence emission ratio was calculated by dividing values measured at the PE maximum (565-575 nm) to the PC maximum (645-655 nm).

D1 protein and β-chain phycoerythrin immunoblotting

Cell pellets were resuspended in extraction buffer (140 mM Tris base, 105 mM Tris-HCl, 0.5 mM ethylenediaminetetraacetic acid, 2% lithium dodecyl sulphate, 10% glycerol and 0.1 mg mL^{-1} PefaBloc protease inhibitor; Roche, Basel, Switzerland) and lysed applying

freezing/thawing cycles and sonication. After centrifugation, total protein concentration was determined using a Lowry protein assay kit and bovine serum albumin as protein standard (Bio-Rad, Hercules, CA). Samples were then denaturated by heating for 2 min at 80 °C in the presence of 50 mM dithiotreitol and an amount of 4 (PsbA protein) or 8 (β-chain PE) µg total protein was loaded on a 4–12% acrylamide gradient precast NuPAGE Bis-Tris mini-gel (Invitrogen, Carlsbad, CA, USA). Gels were electrophoresed and the proteins were transferred onto a polyvinylidene fluoride (PVDF) membrane, then immediately immersed into Tris Buffer Saline-Tween (TBS-T) buffer, pH 7.6 (0.1% Tween 20, 350 mM sodium chloride, 20 mM Trizma base) containing 2% (w:v) blocking agent (Amersham Biosciences, Piscataway, NJ) for 45 min. Aliquots of rabbit primary antibodies against β-subunit PE proteins (directed against the β-subunit PE of *Prochlorococcus* sp. SS120; courtesy of Wolfgang R. Hess, University of Freiburg, Germany; Six *et al*. 2007b, Hess *et al.* 1999) or PsbA (D1 protein; Agrisera) were diluted at 1:50,000 in TBS-T in the presence of 0.5% blocking agent and membranes were soaked into this solution for 1 h with agitation. After extensive washing of the membrane with TBS-T buffer, anti-rabbit secondary antibodies (Biorad) were applied with the same procedure as for primary antibodies. Membranes were developed by chemoluminescence using the ECL Advance reagent kit (Amersham Biosciences) and visualized with a LAS4000 imager equipped with a CCD camera (GE Healthcare).

Pigment analyses

After extraction in 100% methanol, pigment extracts were supplemented with 10% water in order to avoid peak distortion. Hydrophobic pigments were then measured by high pressure liquid chromatography using an HPLC 1100 Series System (Hewlett-Packard, St Palo Alto, CA, USA), equipped with a Kromasil C_8 column (150 x 4.6 mm, 3.5 µm particles size) according to a procedure published elsewhere (Six *et al.* 2005).

Phylogenetic analyses

petB sequences of *Synechococcus* strains obtained from the Roscoff Culture Collection (RCC, http://www.sb-roscoff.fr/Phyto/RCC/) were amplified as previously described (Mazard *et al.* 2012a). Briefly, 550 bp *petB* fragments from MVIR-16-1 (RCC2570), MVIR-11-1 (RCC1695), MVIR-7-1 (RCC1648), MVIR-18-1 (RCC2385), MVIR-16-2 (RCC3010), MVIR-10-1 (RCC1688), MVIR-1-1 (RCC1708) and A15-44 (RCC2527) were amplified directly from cultures at an annealing temperature of 55°C. Sequences were deposited in the GenBank nucleotide sequence database under the accession numbers mentioned in Table S2. A multiple alignment of 74 sequences from cultured isolates was generated with MAFFT v6.818 using the G-INS-I option (Katoh and Toh 2008) and trimAL 1.4 to remove poorly aligned regions and gaps (Capella-Gutiérrez *et al.* 2009). Phylogenetic reconstructions were performed on 559 aligned amino acids using three different methods: maximum likelihood (ML), Bayesian inference and neighbor-joining (NJ). NJ analyses were performed using Phylip 3.69 (Felsenstein 1989) as previously described (Mella-Flores *et al.* 2011). The phylogenetic inference by ML was performed with the Message Passing Interface (MPI) version of PhyML v3.0 (Guindon and Gascuel 2003) using the TrN+I+G, a submodel of the general time-reversible (GTR), with invariant sites and gamma distribution. This model was selected using JModeltest 2.1.3 according the Akaike Information Criterion (Darriba *et al.* 2012). Bayesian inference was conducted using MrBayes 3.1.2 after partitioning according to the position in the codon (Huelsenbeck and Ronquist 2001). Four Markov Chain Monte Carlo (MCMC) simulations were run for five millions generations that were sampled every 100 generations, the first 12500 trees being discarded. The topology of the tree was obtained after ML analyses and the robustness of inferred topologies was supported by 1000 non parametric bootstrap samplings for ML and NJ.

Field temperature data collection

Average sea surface temperature at the strain isolation sites (resolution of 5° squares) and at the month and year of collection were determined using the satellite data available from the National Oceanic and Atmospheric Administration (NOAA, http://iridl.ldeo.columbia.edu/SOURCES/.NOAA/.NCEP/.EMC/.CMB/.GLOBAL/.Reyn_SmithOIv2/.monthly/.sst/). Regarding strains isolated before 1981 (Table S2) for which satellite data are not available, we used the seasonal average temperature at the isolation site (grid of 5° squares) over 10 years (2002-2012). For the strain for which isolation date is not available, *Synechococcus* sp. SYN20, we used the annual average surface seawater temperature over the 10 years. Seawater thermal amplitude at the isolation sites were estimated through the difference between summer and winter average temperature over the 10 years.

Results

Photophysiological differences among the* Synechococcus *strains

When grown in identical conditions at 22°C, the six strains exhibited PSII quantum yields close to 0.6, indicating efficient photosynthetic activity (Table 2). The parameters related to the light-harvesting system showed nevertheless significant differences. The emission spectra indeed displayed a number of strain specificities, including the wavelengths of the maxima, the relative width of the emission bands and the PE to PC ratio (hereafter PE:PC) that ranged from 2.0 to 3.5 (Table 2 and Fig. S1). Furthermore, the amplitude of the state transition process, as estimated by the NPQ_{ST} parameter (see methods), varied significantly among strains from 0.2 to 0.5. *Synechococcus* sp. M16.1 showed weak state transitions with a fairly high fluorescence PE:PC, while *Synechococcus* spp. WH7803 and MVIR-18-1 displayed strong state transitions and a low PE:PC. The most striking differences

among the six strains lied in their pigment cell contents. The tropical *Synechococcus* spp. A15-37 and M16.1 displayed the lowest membrane pigment (Chl *a*, β-carotene and zeaxanthin) contents while it was significantly higher in the mid-latitude strains WH7803 and ROS8604 (Table 2). Similar trends were observed for flow cytometric fluorescence signals with *Synechococcus* sp. A15-37 emitting weak orange fluorescence in contrast to WH7803 and ROS8604 cells, which were brightly fluorescent.

Variations of cell density and fluorescence upon cold stress

In order to highlight possible differences in temperature stress response, cultures fully acclimated to 22°C were shifted to 13°C. The time-course variations of cell abundances differed significantly between the six strains (Fig. 2A). For the tropical strain *Synechococcus* sp. M16.1, the cell density slightly increased after one day, then dramatically dropped down to 2% of the initial cell density after six days of cold stress. In the cultures of strains A15-37 and WH7803, the cell density decreased by half after six days. For *Synechococcus* sp. ROS8604, cell density increased during the first three days, reaching 140% of the initial cell density and then started to decrease. For these four strains, cell density kept decreasing if the cold stress was prolonged over six days (data not shown). By contrast, the two high latitude strains, *Synechococcus* spp. MVIR-16-2 and MVIR-18-1, exhibited significant growth (0.40 ± 0.04 d^{-1} and 0.16 ± 0.03 d^{-1}, respectively), which was comparable to acclimated cultures at 13°C. The former strain reached stationary phase after four to five days at 13°C. As classically observed in stationary phase cultures, drastic physiological changes occurred in the culture, including a drop of the F_M fluorescence level and an increase of the PE fluorescence yield (see below). As this downregulation of photosynthesis is under no circumstances related to a temperature effect and could lead to misinterpretation, data

subsequent to the fourth day are not shown in the following results for *Synechococcus* sp. MVIR-16-2.

Red fluorescence per cell, a proxy for chl *a* cell content, was measured by flow cytometry (Fig. S2A). This parameter decreased down to about 30% of the initial value in the strains isolated at low latitude. In *Synechococcus* sp. ROS8604, the red fluorescence per cell kept fairly stable until the third day and then dropped sharply. In the northern strains, this parameter slightly decreased and stabilised to a level corresponding at about 80% of the initial values. After the temperature shift, all strains reduced their orange fluorescence by about 50% (Fig S2B).

Phycobiliprotein coupling upon cold stress

Fluorescence emission spectra were recorded for each strain at each time point, and used to calculate the PE to PC fluorescence emission ratio (Fig. 2B). This parameter rapidly increased for the low latitude strains *Synechococcus* spp. A15-37 and M16.1, most likely due to an increase of leaking energy between PE and PC, therefore indicating a lower coupling of the PBS rod phycobiliproteins (Six *et al.* 2007b). This process was particularly notable for the tropical *Synechococcus* sp. M16.1, which exhibited a 5.5 fold increase after four days of cold stress. The PE:PC decrease during the last days of the cold period indicates PE degradation, which was also suggested by the bleaching of the cultures at this stage of the experiment. The PE:PC increase was moderate and immediate for strain WH7803, and delayed for ROS8604, starting at the fourth day. The high latitude strains did not show any variation of the PE to PC ratio. Very similar trends were observed among the six strains for the PE to PBS terminal acceptor ratio (data not shown; Fig. S1).

State transition amplitude upon cold stress

We used the non photochemical quenching of fluorescence associated to state transitions, NPQ_{ST}, as an index of the amplitude of this process, which balances the distribution of light energy between the two PS. This mechanism was dramatically affected by low temperature in all *Synechococcus* strains considered, except for the high latitude strains MVIR-16-2 and MVIR-18-1, which showed a lesser decrease of this parameter (45% and 20% of initial condition, respectively; Fig. 3A). State transitions were totally inhibited after one to two days of cold stress in the low latitude strains. In *Synechococcus* spp. WH7803 and ROS8604, NPQ_{ST} decreased progressively to reach a minimal level after four days of cold stress (Fig. 3A).

The recovery capacities of temperate and tropical strains were estimated by placing the cultures back to the initial temperature (22°C, Table S1). The tropical strain A15-37 could never recover from the cold stress and its western counterpart, M16.1, needed more than thirteen days to recover its photosynthetic parameters, and thereafter growth. *Synechococcus* spp. WH7803 and ROS8604 recovered more than twice faster than M16.1.

Photosystem II quantum yield upon cold stress

Upon a 9°C downward temperature shift, we observed a gradient of photosynthetic responses among the six *Synechococcus* strains (Fig. 3B). The PSII quantum yield (F_V/F_M) of the strains isolated at low and medium latitude was dramatically affected by low temperature. *Synechococcus* spp. A15-37 and M16.1 reached minimal yield values after two to three days of cold stress, with very low fluorescence signal after a couple of days. The fluorescence signal of the intermediate latitude strains reached minimum values more slowly, after four to five days. By contrast, strains isolated at high latitude, MVIR-16-2 and MVIR-18-1, suffered only a moderate decrease of the PSII quantum yield, reaching a steady state of *ca* 0.4 after two days. Similarly reduced F_V/F_M (and NPQ_{ST}) values were observed for

both strains once acclimated for several weeks to 13°C (not shown), suggesting that these cultures had already reached an acclimated level for these parameters after four to five days at 13°C.

Time-course relative variations of β-subunit phycoerythrins and D1 protein

Immunoreactions on whole cell proteins using antibodies directed against PE β-subunits and D1 allowed analyzing the variations of the relative quantity of these proteins during the cold stress experiment (Fig. 4). Both antibodies gave clean immunoblots with no parasite bands. The antibody raised against PE β-subunits cross-reacted with both CpeB (PEI) and MpeB (PEII), as previously tested on purified PE (Six *et al.* 2007). In all marine *Synechococcus* genomes, CpeB (~19.1 kDa) is systematically heavier than MpeB (~18.5 kDA). Therefore, the immunoblot profiles often showed two bands whose intensity reflected the quantity of CpeB or MpeB proteins relative to total proteins (Fig. 4A). The intensity of the bands cannot be compared across strains or between subunits because the affinity of the antibody differs depending on aminoacid sequences.

In the tropical strains *Synechococcus* A15-37 and M16.1, cold stress primarily induced MpeB degradation, as indicated by the disappearance of the lower band. CpeB variations were more variable but there was no such strong degradation. In *Synechococcus* spp. WH7803 and ROS8604, the two PE bands were less well separated but a general decreasing trend was clearly observed. In the northern strains, no PE degradation was observed.

We also investigated the relative quantity variations of the D1 protein (~32 kDa), encoded by the *psba* gene family, during the cold period. The cellular pool of this reaction centre II protein decreased rapidly in tropical strains, the signal being hardly detectable after day 3. The D1 band was progressively reduced in mid-latitudes strains *Synechococcus* WH7803 and ROS8604 until quasi disappearance at day 5. In the high latitude strains, MVIR-

16-2 and MVIR-18-1, the D1 relative quantity remains fairly constant along the stress experiment.

Time-course variations of pigment cell content upon cold stress

HPLC pigment analyses revealed the occurrence of three major pigments identified as chl *a*, β-carotene and zeaxanthin, as classically observed in marine *Synechococcus* (see e.g. Kana *et al.* 1988, Six *et al.* 2004), along with minor xanthophylls such as β-cryptoxanthin. The low latitude strains showed a pronounced decrease of the β-carotene to chl *a* ratio, which reached zero at about the fifth day of stress (Fig.5). The mid-latitude strains exhibited different pigment responses to thermal stress. While *Synechococcus* sp. WH7803 underwent a decrease of about 50% of its initial β-carotene to chl *a* ratio, low temperature induced a notable increase of this ratio in *Synechococcus* sp. ROS8604 by a factor two at the fourth day. The large increase of this ratio while the chl *a* fluorescence per cell (reflecting chl *a* cell content) remains unchanged indicates a synthesis of β-carotene. In contrast, the two northern strains did not show any clear trends in the variations of the β-carotene to chl *a* ratio, which remained fairly constant.

We also measured the variations of the zeaxanthin to chl *a* ratio (not shown). While this ratio moderately increased in northern strains due to a decrease in chl *a* cell content (see whole cell chl *a* fluorescence; Fig. S2A), no obvious variation was observed in the three lower latitude strains, indicating a similar degradation rate of the two pigments.

Growth rates vs.temperature

In order to define their temperature optima for growth and compare their thermal growth range in our culture conditions, strains were acclimated to a wide range of temperatures (Fig. 6). The strains showed quite different acclimation capabilities to

temperature. We were able to acclimate *Synechococcus* spp. A15-37 and M16.1, both isolated at latitude lower than 30°N, at temperatures ranging from 18°C to 35°C, with a maximum growth rate about 32°C. These strains exhibited different maximal growth rates, with *Synechococcus* sp. A15-37 growing more slowly than M16.1 (1.70 ± 0.03 d^{-1} and 2.02 ± 0.08 d^{-1} at 32°C, respectively). Despite a similar pattern to M16.1 with a high maximal growth rate value of 2.50 ± 0.08 d^{-1} at 34°C, *Synechococcus* sp. WH7803 could however grow at lower temperatures than the two tropical strains. For the three above-mentioned strains, growth rate sharply decreased at 35°C. We managed to acclimate the strain ROS8604 within a thermal range from 18°C to 30°C, with an optimal temperature at 26°C, corresponding to a growth rate value of 0.83 ± 0.02 day^{-1}. At last, strains MVIR-16-2 and MVIR-18-1, isolated near the polar circle, showed thermal niches shifted toward lower temperatures, MVIR-18-1 being able to cope with temperature down to 10°C (and probably less) and 12°C for MVIR-16-2, but none of these two strains were able to acclimate at temperature higher than 25°C. Furthermore, similar optimal temperatures were observed for the two northern strains, with *Synechococcus* sp. MVIR-16-2 and MVIR-18-1 growing optimally at about 22°C (1.00 ± 0.04 day^{-1} and 0.82 ± 0.07 day^{-1}, respectively).

Phyloecology of marine* Synechococcus *isolates

In order to unveil potential relationships between *Synechococcus* phylogeny and the temperature of strain isolation site, a phylogenetic analysis was conducted on the *petB* sequence of 74 cultured strains isolated from a wide range of latitudes, across different oceans and seas (Fig. 7, Table S2). This marker was chosen because it provides a better phylogenetic resolution of *Synechococcus* strains (at the subclade level) than more typical markers, such as 16S rRNA or ITS (Mazard *et al.* 2012a). Our data set includes a number of strains from the Roscoff Culture Collection, whose phylogenetic position was so far

unknown, in particular strains isolated during the MICROVIR cruise (July 2007, North Sea ; Table S2). The data set mainly included representatives of subcluster 5.1 and the phylogenetic tree was rooted with one representative of each of the two other subclusters (5.2 and 5.3; *sensu* Dufresne et al., 2008). As in a previous study using the *petB* gene (Mazard *et al.* (2012a), members of subcluster 5.1 were divided into eleven clades and a number of these clades were further subdivided into 14 sub-clades (Fig. 7). It is worth noting that we found a slight difference with regard to Mazard and coworkers' study concerning sub-clade Ib, which does not constitute a monophyletic group in our analysis. This disparity is probably imputable to the differences in the phylogenetic methods used between the two studies. This tree allowed us to assign the tropical *Synechococcus* spp. A15-37 and M16.1 to subclade IIa, *Synechococcus* spp. ROS8604, MVIR-16-2 and MVIR-18-1 to sub-clade Ia, while *Synechococcus* sp. WH7803 is one of the rare representatives of clade V available in culture.

In parallel to the phylogenetic analyses, the average seawater temperatures at the isolation sites were retrieved for the 74 strains. Comparison between the phylogeny and the average isolation temperatures underlined that clades I and IV strains were isolated in significantly colder waters (15.03 ± 2.53°C and 15.05 ± 2.13°C respectively) than the isolates from clades II and III (23.93 ± 3.03°C and 24.86 ± 2.84°C respectively), as shown by one-way ANOVA ($F = 36.26$, p-value < 0.01).

Discussion

In this study, we compare the physiology of six marine *Synechococcus* strains isolated at different latitudes (from 23°N to 61°N; Table 1; Fig.1) in near coastal areas (*i.e.* mesotrophic waters) of the North Atlantic Ocean. All of them belong to pigment type 3a (Six *et al.* 2007c, Humily *et al.* in press), but in spite of this similar PBS composition, the six strains

exhibited large differences in pigment cell content (chl *a*, carotenoids and PE; Table 2), with the mid-latitude strains being much more pigmented than their northern and tropical counterparts. These sharp differences are probably associated with different thylakoidal surfaces per cell and/or different cell biovolumes among strains. Moreover, whereas fluorescence excitation spectra were quite comparable, fluorescence emission spectra showed differences in wavelength maxima, maxima ratios and apparent width of the PE emission band (Fig. S1), revealing the occurrence of distinct levels of PBP coupling. These six strains, which display very similar fluorescence PUB to PEB ratio (ca 0.4), could thus be differentiated by other photosynthetic features (Table 2). These observations highlight the functional microdiversity that exists within the marine *Synechococcus* pigment types defined in previous studies (Six *et al.* 2007c, Humily *et al.* in press).

Marine* Synechococcus *show differential resistance to cold stress

Cold stress experiments revealed large differences in thermal flexibility among the six marine *Synechococcus* strains used in this study. Whereas tropical strains were not able to stand the temperature drop challenge, the temperate strains maintained a nearly constant cell density (Fig. 2A). By contrast, the northern strains kept dividing, at similar growth rates than cells fully acclimated to 13°C (Fig. 2A). In these photosynthetic organisms, being able to sustain efficient light absorption capacities and utilization is crucial for growth. In order to better understand the differences among the strains, we first followed the response of their photosynthetic antenna, the PBS, during the cold period (Fig. 2B, 4A). In contrast to the northern strains, for which PBS fluorescence spectra and PE cell content remained fairly constant, the strong increase in PE:PC fluorescence ratio observed in *Synechococcus* spp. A15-37, M16.1, WH7803 and ROS8604 indicates an impairment of the phycobiliprotein coupling, which likely led to the physical disconnection of PE molecules from the rest of the

PBS structure (Six *et al.* 2007b). PBS impairment was especially severe for *Synechococcus* sp. M16.1, for which fast specific degradation of the distal PBS hexamers (PEII) was evidenced by MpeB immunobloting (Fig. 4A). Our results are comparable to previous studies led in other cyanobacteria that pointed out serious PBS perturbations in response to UV (Lao and Glazer 1996, Rajagopal and Murthy 1996, Rinalducci *et al.* 2006, Six *et al.* 2007b), high light (Tamary *et al.* 2012) and temperature stress (Li *et al.* 2001, Stoitchkova *et al.* 2007), and thus suggests that PBS uncoupling and dismantling is a usual consequence of environmental stress in cyanobacteria. It is however worth noting that the highly fluorescent free PE may also constitute a way of energy dissipation through fluorescence during a stress period. In any case, the cold-induced destruction of the antenna considerably decreased cell absorption capacities and must have had a strong impact on the growth capacities of the temperate and tropical strains studied here.

Cyanobacteria balance excitation energy notably through PBS state transitions, which regulate the energy transfer from PBS to PSI and PSII in response to environmental factors or metabolism demands (Joshua and Mullineaux 2004, Mullineaux and Emlyn-Jones 2004). The drastic decrease observed in state transitions amplitude during cold shock for the tropical and mid-latitude strains generally arose before the PBS uncoupling in these strains, indicating that the decline in state transition during the first few days was not directly related to PBS dismantling (Fig. 2B, 3A). These early perturbations of the state transition process might originate in the cold-induced changes in the fluidity of the thylakoidal membranes, as low temperature is well known to induce membrane stiffening (Wada and Murata 1990, Murata and Los 1997, Mikami and Murata 2003). Later during the cold period, PBS dismantling likely contributes to the complete inhibition of state transitions. The high latitude *Synechococcus* strains, spp. MVIR-16-2 and MVIR-18-1 showed much better

capacities to regulate state transitions, possibly through active regulation of thylakoid fluidity (Murata and Wada 1995, Murata and Los 1997).

The PSII quantum yield (F_V/F_M) is a good proxy for the efficiency with which the reaction center II converts the energy funneled by the PBS into electron flux. The most likely explanation for the major non-reversible decrease of the PSII quantum yield during cold stress in tropical and temperate strains is the photoinactivation of the reaction center II (for review see e.g. Campbell and Tyystjärvi 2012). This phenomenon is unavoidably induced by light in any oxygenic photosynthetic organism but is further accelerated by environmental stresses that disturb the balance between light absorption and utilization, such as temperature variations (Takahashi and Murata 2008). Cold stress is indeed thought to decrease the repair rate of the D1 protein, the key protein of the PSII reaction center, thus inducing the concomitant drop in D1 cell content and PSII quantum yield reported in the sensitive strains (Fig. 3B and 4B). The observation that high-latitude strains did not suffer from PSII inactivation during the cold period raise questions about the physiological processes that allow such tolerance, and calls for further research.

Cold stress, protection and acclimation

To counteract the photoinhibition induced by reduced metabolic rates at low temperature (Burns *et al.* 2005), reversible physiological adjustments are induced by photosynthetic organisms, referred as photoacclimation. Acclimation of the photosynthetic apparatus to low temperature usually shows strong similarities to high light acclimation processes (Oquist 1983, Maxwell *et al.* 1994, Huner *et al.* 1998), as it is also based on an imbalance between light energy absorption and its downstream utilization. We indeed observed in the northern strains hints of high light-like acclimation (see e.g. Six *et al.* 2004, 2005), such as a reduction in pigment fluorescence per cell (Fig. S2) and chl *a* (data not

shown), likely associated with the reduction of the thylakoïdal surface (Kana and Glibert 1987).

The PSII quantum yield of the northern strains decreased until a level close to that measured in cultures fully acclimated to 13°C (not shown), while the D1 cell content kept stable (Fig 4B). This suggests the induction of non photochemical quenching associated with light energy dissipation, characterised by a reduction of the amount of energy processed by the reaction center (for review see Campbell *et al.* 1998; Kirilowski and Kerfeld 2012, 2013). The results thus suggest that, in contrast to the tropical and mid-latitude strains, the northern ones managed to adjust their light utilization capacities to the cold-induced slowing down of their metabolism, an ability which likely limits the formation of reactive oxygen species (Asada 1994, Latifi *et al.* 2009). In cyanobacteria, the best known non photochemical quenching mechanism associated with light energy dissipation involves the so-called orange carotenoid protein, encoded by the *ocp* gene, which seemingly acts as a photoreceptor and intercepts light energy at the PBS core, before it reaches reaction center II (Wilson *et al.* 2006, Kirilovsky and Kerfeld 2012). The effects of cold stress on the activity of this protein, whose gene is present in most marine *Synechococcus* strains (Scanlan *et al.* 2009), remain to be studied.

A number of β-carotene molecules bound to the reaction center II act as quenchers of singlet oxygen and under light, are regenerated through a repair cycle (Telfer 2005, Ishikita *et al.* 2007, Mella-Flores *et al.* 2012). This carotenoid is essential for the protection of reaction centers (Cazzaniga *et al.* 2012) and thus may be used as an indicator of oxidative stress intensity. The β-carotene measurements revealed that tropical strains suffered from strong oxidative stress during the cold period (Fig. 5). The sharp degradation of β-carotene, probably due to an impairment of the turnover of this antioxidant, observed for *Synechococcus* spp. A15-37, M16.1 and to a lesser extent WH7803, implies that the PSII of

these strains were subjected to direct oxidative damages (Blot *et al.* 2011). Furthermore, oxidative stress is also thought to prevent the repair of the PSII key protein, D1 (Nishiyama *et al.* 2006), thus greatly enhancing PSII inactivation. Interestingly, *Synechococcus* sp. ROS8604 responded differently, as it transiently increased its β-carotene cell content until the fourth day of stress, probably by boosting the β-carotene cycle. This rapid synthesis likely allowed a better protection against oxidative stress and may partially explain the moderate growth of this strain at the beginning of the cold period (Fig. 2A). However, cultures of *Synechococcus* sp. ROS8604 eventually did not manage to cope with oxidative stress, as seen by the rising of PBS uncoupling (Fig. 2B) and the cell density decrease (Fig. 2A), starting from the fourth day of stress. Variability in carotenoid response to temperature has also been observed among cyanobacterial strains isolated from high latitude freshwaters (Tang *et al.* 1997).

Differences in cold resistance capacities were also noticeable when considering the recovery capacities (Table S1). *Synechococcus* sp. M16.1 needed much longer time to recover and the cold period turned out to be lethal for *Synechococcus* sp. A15-37. The WH7803 and ROS8604 strains were not able to maintain growth and photosynthetic activity during the cold period, but they both recovered quite quickly when replaced to initial temperature, indicating significant thermal flexibility. These strains thus appear quite well adapted to temperate environments, in which temperature fluctuate depending on the seasons.

Marine Synechococcus *strains have different thermal* preferenda

The different physiological responses of the six marine *Synechococcus* strains to cold stress are associated with distinct long-term acclimation capacities to different temperatures. Our study thus demonstrates for the first time that marine *Synechococcus* strains exhibit different thermal *preferenda* and, therefore, strongly suggests the existence

of strains adapted to different local temperature ranges. These preferences appear to be related to the latitude of isolation of each strain, which is directly linked to the latitudinal gradient of seawater temperature. The temperature *vs.* growth curve of the WH8103 strain, isolated in the Sargasso Sea at 28.5°N, exhibits a maximum at 28°C (Moore *et al.* 1995) and thus supports this conclusion. Our observations support recent surveys which stated that optimum temperature for growth of marine phytoplankton strains is related to the latitude and temperature of their isolation site (Thomas *et al.* 2012, Boyd *et al.* 2013), and support field observations that the abundances of the *Synechococcus* of the 5.1 cluster fall to very low values in the polar oceans, of about hundred cells per mL (Gradinger and Lenz 1995, Vincent 2000, Not *et al.* 2004, Cottrell and Kirchman 2009, Vincent and Kesada 2012).

The two northern *Synechococcus* strains we studied cannot be considered as true psychrophilic organisms but rather as psychrotolerant ones (Tang *et al.* 1997). Indeed, although strains such as *Synechococcus* sp. MVIR-18-1 (one of the culture isolates which, to our knowledge, shows the northernmost isolation latitude) can probably survive at temperature below 10°C, true psychrophilic phytoplankton exhibit optimal temperature lower than 15°C and can generally not grow over 20°C (Vincent 2000, Lovejoy *et al.* 2007). Although we cannot exclude the existence of true psychrophilic strains within the *Synechococcus* 5.1 group, as it might be the case for natural *Synechococcus* subcluster 5.2 populations (Cottrell and Kirchman 2009, Huang *et al.* 2011), it appears that northern 5.1 strains might have only moderately decreased their optimal temperature during the evolution and acquired the capacity to stand low temperatures.

Our results suggest that the capacity to grow at low temperature may only be possible to the detriment of the ability to develop high growth rates, as observed for the low latitude strains A15-37, M16.1 and WH7803 (Fig. 6). This apparent trade-off between growth performances and the capacity to grow over a given temperature range, which has also been

observed for *Prochlorococcus* picocyanobacteria (Johnson *et al.* 2006), might constitute a general adaptative trait of marine picocyanobacteria to different thermal niches. In addition, it is worth noting that *Synechococcus* strains display shapes of the growth *vs.* temperature curves similar to *Prochlorococcus* ecotypes (Johnson *et al.* 2006, Moore *et al.* 1995). The typical shoulder in the first part of the curve (Fig. 6) may reflect the triggering of a thermophysiological mechanism that allows efficient acclimation to higher temperature, a mechanism that was possibly lost by the northern strains.

Marine* Synechococcus *display temperature specialized clades

The combination of phylogenetic analyses of a large number of *Synechococcus* culture isolates (Fig. 7; Table S2) with their isolation temperatures provides an interesting complement to the field studies of Zwirglmaier and coworkers (2007, 2008). This approach allowed us to highlight differences in the thermal niches of some of the *Synechococcus* clades. Laboratory strains belonging to clades I and IV were isolated in colder waters than those from clade II and III (Fig. 7). This result is coherent with the latitudinal distribution of the *Synechococcus* clades, as field studies reported that clades I and IV are generally confined to latitudes higher than 30° N/S. The two other dominant clades II and III seem to prevail in the warmer waters of the warm temperate and tropical/sub-tropical regions of the ocean (Zwirglmaier *et al.* 2007, 2008, Huang *et al.* 2011). It should be noted that strains CC9605 (clade III) and A15-11 (clade II), for which temperature isolation was below 19°C, were collected in upwelling areas (California current and Mauritania coast, respectively) where water temperature is usually colder and more variable. Strains from clade VI seem to be easily brought to culture, as shown by the relatively high number of isolates available in culture collections (data not shown), but are not very abundant in the field (Huang *et al.* 2011). The wide spectrum of temperature at which these strains have been isolated (Fig. 7)

suggests that clade VI might gather strains with high physiological flexibility regarding temperature.

The temperature adaptation capacities of the six strains considered in this study are in line with their phylogenetic position. The tropical strains A15-37 and M16.1, which showed high optimal temperature for growth and could not grow below c.a. 18°C, belong to clade II. Similar observations were made for the clade III strain *Synechococcus* sp. WH8103 (Moore *et al.* 1995). Among the strains we studied, *Synechococcus* spp. ROS8604, MVIR-16-2 and MVIR-18-1 belong to clade I and appear to be the best adapted to cold waters. It is however worth noting that the three strains show differential responses to cold stress (Fig. 2, 3, 4, and 5) and different temperature *preferenda* (Fig. 6), with a good correspondence to their isolation latitude. Thus, clade I *Synechococcus* strains, living at the northernmost limit of distribution (near the polar circle), show better capacities to cope with low temperature than those isolated from cold temperate waters. This highlights the existence of significant functional microdiversity regarding adaptative capacities to temperature within marine *Synechococcus* clade I.

Conclusion

This study demonstrates for the first time that marine *Synechococcus* strains exhibit considerably different physiological capacities to cope with temperature variations and display different thermal *preferenda*. These abilities might rely on the capacities to maintain the photosynthetic apparatus in a state that limits the induction of oxidative stress. Furthermore, our study suggests a correlation between the ability to cope with temperature variations and specific clades of the marine *Synechococcus* radiation. Our results suggest that clade I and probably clade IV *Synechococcus* have a physiology preferentially adapted to cold thermal niches. These observations, which are quite in line with phylogeographic field

studies (Zwirglmaier *et al.* 2007, 2008), suggest the existence of low temperature ecotypes, *i.e.* cold thermotypes, among marine *Synechococcus* and underline an important role of temperature in the diversification of marine *Synechococcus* at least at high latitudes. The deep understanding of the differentiation of cold *Synechococcus* thermotypes at high latitudes will however not be easy, given the functional microdiversity occurring within *Synechococcus* clade I, a diversity which likely reflects adaptation the continuous latitudinal gradient of temperature. Although clade II (and III; Moore *et al.* 1995) cells seem more adapted to warm waters, more work is necessary to evaluate the importance of temperature relative to other environmental factors in the *Synechococus* diversification at lower latitudes.

The absence of comparative data on the thermophysiology of marine *Synechococcus* has so far made it impossible to build predictive models of picocyanobacteria distribution taking in account the thermal flexibility of these organisms (Flombaum *et al.* 2013). As our results suggest that the composition of the *Synechococcus* natural communities may experience major changes in the context of possible climatic changes due to the occurrence of temperature ecotypes, future modeling efforts should incorporate growth rate data in order to better predict the global response of marine *Synechococcus* to environmental changes.

Supplementary information is available at ISMEJ's website.

Acknowledgement

This work was supported by the French program ANR PELICAN (PCS-09-GENM-200), the EMBRC France (INFRA-2010-2.2.5) and the European Union programs MicroB3 and MaCuMBA (grant agreements 287589 and 311975, respectively). We certify that there is no

conflict of interest with any financial organization regarding the material discussed in this manuscript. Justine Pittera was supported by the French Ministry of Higher Education and Research. We warmly thank Frédéric Partensky for improving the manuscript as well as Morgane Ratin for her help with the cultures and the gene sequencing. We are also grateful to the Roscoff Culture Collection for maintaining the *Synechococcus* strains used in this study and in particular to Florence Legall who isolated some them.

Supplementary information is available at ISMEJ's website.

References

Ahlgren NA, Rocap G. (2012). Diversity and distribution of marine *Synechococcus*: multiple gene phylogenies for consensus classification and development of qPCR assays for sensitive measurement of clades in the ocean. *Front Microbiol* **3:** 213-213.

Asada K (1994). Production and action of active oxygen species in photosynthetic tissues. In: Foyer CH, Mullineaux PM (eds). *Causes of photooxidative stress and amelioration of defence systems in plants*. pp 77-104.

Blot N, Mella-Flores D, Six C, Le Corguille G, Boutte C, Peyrat A *et al.* (2011). Light history influences the response of the marine cyanobacterium *Synechococcus* sp. WH7803 to oxidative stress. *Plant Physiol* **156:** 1934-1954.

Boyd PW, Rynearson TA, Armstrong EA, Fu F, Hayashi K, Hu Z *et al.* (2013). Marine phytoplankton temperature versus growth responses from polar to tropical waters – Outcome of a scientific community-wide study. *PLoS ONE* **8:** e63091.

Buitenhuis ET, Li WKW, Vaulot D, Lomas MW, Landry M, Partensky F *et al.* (2012). Picophytoplankton biomass distribution in the global ocean. *Earth System Science Data* **4:** 37-46.

Burns RA, MacDonald CD, McGinn PJ, Campbell DA. (2005). Inorganic carbon repletion disrupts photosynthetic acclimation to low temperature in the cyanobacterium *Synechococcus* elongatus. *J Phycol* **41:** 322-334.

Campbell D, Hurry V, Clarke AK, Gustafsson P, Oquist G. (1998). Chlorophyll fluorescence analysis of cyanobacterial photosynthesis and acclimation. *Microbiol Mol Biol Rev* **62:** 667-683.

Campbell DA, Tyystjärvi E. (2012). Parameterization of photosystem II photoinactivation and repair. *Biochim Biophys Acta, Bioenerg* **1817:** 258-265.

Capella-Gutiérrez S, Silla-Martinez JM, Gabaldon T. (2009). trimAl: a tool for automated alignment trimming in large-scale phylogenetic analyses. *Bioinformatics* **25:** 1972-1973.

Cazzaniga S, Li Z, Niyogi KK, Bassi R, Dall'Osto L. (2012). The *Arabidopsis* szl1 mutant reveals a critical role of beta-carotene in photosystem I photoprotection. *Plant Physiol* **159:** 1745-1758.

Cottrell MT, Kirchman DL. (2009). Photoheterotrophic microbes in the Arctic ocean in summer and winter. *Appl Environ Microbiol* **75:** 4958-4966.

Darriba D, Taboada GL, Doallo R, Posada D. (2012). jModelTest 2: more models, new heuristics and parallel computing. *Nature Methods* **9:** 772-772.

Felsenstein J. (1989). PHYLIP - Phylogeny Inference Package (Version 3.2). *Cladistics* **5:** 164-166.

Flombaum P, Gallegos JL, Gordillo RA, Rincón J, Zabala LL, Jiao N *et al.* (2013). Present and future global distributions of the marine cyanobacteria *Prochlorococcus* and *Synechococcus*. *Proc Natl Acad Sci* **110:** 9824-9829.

Fu F-X, Warner ME, Zhang Y, Feng Y, Hutchins DA. (2007). Effects of increased temperature and CO2 on photosynthesis, growth, and elemental ratios in marine *Synechococcus* and *Prochlorococcus*. *J Phycol* **43:** 485-496.

Fuller NJ, Marie D, Partensky F, Vaulot D, Post AF, Scanlan DJ. (2003). Clade-specific 16S ribosomal DNA oligonucleotides reveal the predominance of a single marine *Synechococcus* clade throughout a stratified water column in the Red Sea. *Appl Environ Microbiol* **69:** 2430-2443.

Fuller NJ, West NJ, Marie D, Yallop M, Rivlin T, Post AF *et al.* (2005). Dynamics of community structure and phosphate status of picocyanobacterial populations in the Gulf of Aqaba, Red Sea. *Limnol Oceanogr* **50:** 363-375.

Gradinger R, Lenz J. (1995). Seasonal occurrence of picocyanobacteria in the Greenland Sea and central Arctic Ocean. *Polar Biol* **15:** 447-452.

Guindon S, Gascuel O. (2003). A simple, fast, and accurate algorithm to estimate large phylogenies by maximum likelihood. *Syst Biol* **52:** 696-704.

Herdman M, Castenholz RW, Waterbury JB, Rippka R (2001). Form-genus XIII. *Synechococcus*. In: Boone DR, Castenholz RW (eds). *Bergey's Manual of Systematic Bacteriology*, 2d Ed. edn. Springer-Verlag: New York. pp 508-512.

Hess WR, Steglich C, Lichtlé C, Partensky F (1999). Phycoerythrins of the oxyphotobacterium *Prochlorococcus marinus* are associated to the thylakoid membrane and are encoded by a single large gene cluster. *Plant Mol Biol* **40**: 507-521.

Huang S, Wilhelm SW, Harvey HR, Taylor K, Jiao N, Chen F. (2011). Novel lineages of *Prochlorococcus* and *Synechococcus* in the global oceans. *ISME J* **6:** 285-297.

Huelsenbeck JP, Ronquist F. (2001). MRBAYES: Bayesian inference of phylogenetic trees. *Bioinformatics* **17:** 754-755.

Humily F, Partensky F, Six C, Farrant G, Ratin M, Marie D *et al.* (submitted). A gene island with dual evolutionary origin is involved in chromatic acclimation in marine *Synechococcus*. *PLoS One* in press.

Huner NPA, Oquist G, Sarhan F. (1998). Energy balance and acclimation to light and cold. *Trends Plant Sci* **3:** 224-230.

Ishikita H, Loll B, Biesiadka J, Kern J, Irrgang K-D, Zouni A *et al.* (2007). Function of two beta-carotenes near the D-1 and D-2 proteins in photosystem II dimers. *Biochim Biophys Acta, Bioenerg* **1767:** 79-87.

Johnson ZI, Zinser ER, Coe A, McNulty NP, Woodward EM, Chisholm SW. (2006). Niche partitioning among *Prochlorococcus* ecotypes along ocean-scale environmental gradients. *Science* **311:** 1737-1740.

Joshua S, Mullineaux CW. (2004). Phycobilisome diffusion is required for light-state transitions in cyanobacterial. *Plant Physiol* **135:** 2112-2119.

Kana TM, Glibert PM. (1987). Effect of irradiances up to 2000 µE m^{-2} s^{-1} on marine *Synechococcus* WH7803—I. Growth, pigmentation, and cell composition. *Deep Sea Research Part A Oceanographic Research Papers* **34:** 479-495.

Kana TM, Glibert PM, Goericke R, Welschmeyer NA. (1988). Zeaxanthin and beta-carotene in *Synechococcus* WH7803 respond differently to irradiance. *Limnol Oceanogr* **33:** 1623-1627.

Katoh K, Toh H. (2008). Improved accuracy of multiple ncRNA alignment by incorporating structural information into a MAFFT-based framework. *BMC Bioinfo* **9:** 212.

Kirilovsky D, Kerfeld CA. (2012). The orange carotenoid protein in photoprotection of photosystem II in cyanobacteria. *Biochim Biophys Acta, Bioenerg* **1817:** 158-166.

Kirilovsky D, Kerfeld CA. (2013). The orange carotenoid protein: a blue-green light photoactive protein. *Photochem & Photobiol Sci* **12**: 1135-1143.

Lantoine F, Neveux J. (1997). Spatial and seasonal variations in abundance and spectral characteristics of phycoerythrins in the tropical northeastern Atlantic Ocean. *Deep Sea Res, Part I* **44:** 223-246.

Lao K, Glazer AN. (1996). Ultraviolet-B photodestruction of a light-harvesting complex. *Proc Natl Acad Sci* **93:** 5258-5263.

Latifi A, Ruiz M, Zhang C-C. (2009). Oxidative stress in cyanobacteria. *FEMS Microbiol Rev* **33:** 258-278.

Li WKW. (1994). Primary Production of Prochlorophytes, Cyanobacteria, and Eucaryotic Ultraphytoplankton: Measurements from Flow Cytometric Sorting. *Limnol Oceanogr* **39:** 169-175.

Li Y, Zhang JP, Xie J, Zhao JQ, Jiang LJ. (2001). Temperature-induced decoupling of phycobilisomes from reaction centers. *Biochim Biophys Acta, Bioenerg* **1504:** 229-234.

Liu H, Nolla H, Campbell L. (1997). *Prochlorococcus* growth rate and contribution to primary production in the equatorial and subtropical North Pacific Ocean. *Aquat Microb Ecol* **12:** 39-47.

Liu S, Juneau P, Qiu B. (2012). Effects of iron on the growth and minimal fluorescence yield of three marine *Synechococcus* strains (Cyanophyceae). *Phycol Res* **60:** 61-69.

Lovejoy C, Vincent WF, Bonilla S, Roy S, Martineau M-J, Terrado R *et al.* (2007). Distribution, phylogeny, and growth of cold-adapted Picoprasinophytes in Artic sea. *J Phycol* **43:** 78-89.

Marie D, Brussaard C, Partensky F, Vaulot D (1999). Flow cytometric analysis of phytoplankton, bacteria and viruses. In: Sons JW (ed). *Current Protocols in Cytometry*. International Society for Analytical Cytology. pp 11.11.11-11.11.15.

Maxwell DP, Falk S, Trick CG, Huner NPA. (1994). Growth at low-temperature mimics high light acclimation in *Chlorella-vulgaris*. *Plant Physiol* **105:** 535-543.

Mazard S, Ostrowski M, Partensky F, Scanlan DJ. (2012a). Multi-locus sequence analysis, taxonomic resolution and biogeography of marine *Synechococcus*. *Environ Microbiol*.

Mazard S, Wilson WH, Scanlan DJ. (2012b). Dissecting the physiological response to phosphorus stress in marine *Synechococcus* isolates. *J Phycol* **48:** 94-105.

Mella-Flores D, Mazard S, Humily F, Partensky F, Mahe F, Bariat L *et al.* (2011). Is the distribution of *Prochlorococcus* and *Synechococcus* ecotypes affected by global warming? *Biogeosciences* **8:** 2785-2804.

Mella-Flores D, Six C, Ratin M, Partensky F, Boutte C, Le Corguillé G *et al.* (2012). *Prochlorococcus* and *Synechococcus* have evolved different adaptive mechanisms to cope with light and UV stress. *Front Microbiol* **3**.

Mikami K, Murata N. (2003). Membrane fluidity and the perception of environmental signals in cyanobacteria and plants. *Prog Lipid Res* **42:** 527-543.

Moore LR, Goericke R, Chisholm SW. (1995). Comparative physiology of *Synechococcus* and *Prochlorococcus*: influence of light and temperature on growth, pigments, fluorescence and absorptive properties. *Mar Ecol Progr Ser* **116:** 259-275.

Moore LR, Rocap G, Chisholm SW. (1998). Physiology and molecular phylogeny of coexisting *Prochlorococcus* ecotypes. *Nature* **393:** 464-467.

Mullineaux CW, Emlyn-Jones D. (2004). State transitions: an example of acclimation to low-light stress. *J Exp Bot* **56:** 389-393.

Murata N, Wada H. (1995). Acyl-lipid desaturases and their importance in the tolerance and acclimatization to cold of cyanobacteria. *Biochem J* **308:** 1-8.

Murata N, Los DA. (1997). Membrane fluidity and temperature perception. *Plant Physiol* **115:** 875-879.

Nishiyama Y, Allakhverdiev SI, Murata N. (2006). A new paradigm for the action of reactive oxygen species in the photoinhibition of photosystem II. *Biochim Biophys Acta* **1757:** 742-749.

Not F, Latasa M, Marie D, Cariou T, Vaulot D, Simon N. (2004). A single species, *Micromonas pusilla* (Prasinophyceae), dominates the eukaryotic picoplankton in the western English channel. *Appl Environ Microbiol* **70:** 4064-4072.

Not F, Massana R, Latasa M, Marie D, Colson C, Eikrem W *et al.* (2005). Late summer community composition and abundance of photosynthetic picoeukaryotes in Norwegian and Barents Seas. *Limnol Oceanogr* **50:** 1677-1686.

Olson RJ, Chisholm SW, Zettler ER, Armbrust EV. (1990). Pigments, size, and distribution of *Synechococcus* in the North Atlantic and Pacific Oceans. *Limnol Oceanogr* **35:** 45-58.

Oquist G. (1983). Effetcs of low-temperature on photosynthesis. *Plant, Cell Environ* **6:** 281-300.

Palenik B. (2001). Chromatic adaptation in marine *Synechococcus* strains. *Appl Environ Microbiol* **67:** 991-994.

Palenik B, Ren Q, Dupont CL, Myers GS, Heidelberg JF, Badger JH *et al.* (2006). Genome sequence of *Synechococcus* CC9311: Insights into adaptation to a coastal environment. *Proc Natl Acad Sci USA* **103:** 13555-13559.

Partensky F, Blanchot J, Vaulot D (1999). Differential distribution and ecology of *Prochlorococcus* and *Synechococcus* in oceanic waters: a review. *Marine Cyanobacteria*. Bulletin de l'Institut Oceanographique: Monaco. pp 457-475.

Partensky F, Garczarek L. (2010). *Prochlorococcus*: Advantages and limits of minimalism. *Annu Rev Mar Sci* **2:** 305-331.

Post AF, Penno S, Zandbank K, Paytan A, Huse SM, Welch DM. (2011). Long term seasonal dynamics of *Synechococcus* population structure in the gulf of Aqaba, northern Red Sea. *Front microbiol* **2:** 131-131.

Rajagopal S, Murthy SDS. (1996). Short term effect of ultraviolet-B radiation on photosystem 2 photochemistry in the cyanobacterium *Synechococcus* 6301. *Biol Plant* **38:** 129-132.

Rinalducci S, Hideg É, Vass I, Zolla L. (2006). Effect of moderate UV-B irradiation on *Synechocystis* PCC 6803 biliproteins. *Biochem Biophys Res Commun* **341:** 1105-1112.

Rippka R, Coursin T, Hess W, Lichtlé C, Scanlan DJ, Palinska KA *et al.* (2000). *Prochlorococcus marinus* Chisholm et al. 1992 subsp. *pastoris* subsp. nov. strain PCC 9511, the first axenic chlorophyll a_2/b_2-containing cyanobacterium (Oxyphotobacteria). *International Journal of Systematic and Evolutionary Microbiology* **50:** 1833-1847.

Rocap G, Distel DL, Waterbury JB, Chisholm SW. (2002). Resolution of *Prochlorococcus* and *Synechococcus* ecotypes by using 16S-23S ribosomal DNA internal transcribed spacer sequences. *Appl Environ Microbiol* **68:** 1180-1191.

Scanlan, Ostrowski M, Mazard S, Dufresne A, Garczarek L, Hess WR *et al.* (2009). Ecological genomics of marine picocyanobacteria. *Microbiol Mol Biol Rev* **73:** 249-299.

Sherry ND, Wood MA. (2001). Phycoerythrin-containing picocyanobacteria in the Arabian Sea in February 1995: diel patterns, spatial variability, and growth rates. *Deep Sea Res, Part II* **48:** 1263-1283.

Six C, Thomas JC, Brahamsha B, Lemoine Y, Partensky F. (2004). Photophysiology of the marine cyanobacterium *Synechococcus* sp. WH8102, a new model organism. *Aquat Microb Ecol* **35:** 17-29.

Six C, Worden AZ, Rodriguez F, Moreau H, Partensky F. (2005). New insights into the nature and phylogeny of Prasinophyte antenna proteins: *Ostreococcus* tauri, a case study. *Mol Biol and Evol* **22**.

Six C, Finkel ZV, Irwin AJ, Campbell DA. (2007a). Light variability illuminates niche-partitioning among marine picocyanobacteria. *PLoS ONE* **2:** e1341.

Six C, Joubin L, Partensky F, Holtzendorff J, Garczarek L. (2007b). UV-induced phycobilisome dismantling in the marine picocyanobacterium *Synechococcus* sp. WH8102. *Photosynth Res* **92:** 75-86.

Six C, Thomas JC, Garczarek L, Ostrowski M, Dufresne A, Blot N *et al.* (2007c). Diversity and evolution of phycobilisomes in marine *Synechococcus* spp. - a comparative genomics study. *Genome Biol* **8:** R259.

Six C, Sherrard R, Lionard M, Roy S, Campbell DA. (2009). Photosystem II and pigment dynamics among ecotypes of the green alga *Ostreococcus*. *Plant Physiol* **151:** 379-390.

Stoitchkova K, Zsiros O, Javorfi T, Pali T, Andreeva A, Gombos Z *et al.* (2007). Heat- and light-induced reorganizations in the phycobilisome antenna of *Synechocystis* sp PCC 6803. Thermo-optic effect. *Biochim Biophys Acta, Bioenerg* **1767:** 750-756.

Stuart RK, Dupont CL, Johnson DA, Paulsen IT, Palenik B. (2009). Coastal strains of marine *Synechococcus* species exhibit increased tolerance to copper shock and a distinctive transcriptional response relative to those of open-ocean strains. *Appl Environ Microbiol* **75:** 5047-5057.

Takahashi S, Murata N. (2008). How do environmental stresses accelerate photoinhibition? *Trends Plant Sci* **13:** 178-182.

Tamary E, Kiss V, Nevo R, Adam Z, Bernat G, Rexroth S *et al.* (2012). Structural and functional alterations of cyanobacterial phycobilisomes induced by high-light stress. *Biochim Biophys Acta, Bioenerg* **1817:** 319-327.

Tang PY, Tremblay R, Vincent W. (1997). Cyanobacterial dominance of polar freshwater ecosystems : are high-latitude mat-formers adapted to low temperature? *J Phycol* **33**: 171:181

Telfer A. (2005). Too much light? How beta-carotene protects the photosystem II reaction centre. *Photochem Photobiol Sci* **4:** 950-956.

Thomas MK, Kremer CT, Klausmeier CA, Litchman E. (2012). A global pattern of thermal adaptation in marine phytoplankton. *Science* **338:** 1085-1088.

Vaulot D. (1989). CYTOPC: Processing software for flow cytometric data. *Signal and Noise* **2:** 8.

Vaulot D, Le Gall F, Marie D, Guillou L, Partensky F. (2004). The Roscoff Culture Collection (RCC): a collection dedicated to marine picoplankton. *Nova Hedwigia* **79:** 49-70.

Vincent W. (2000). Cyanobacterial dominance in the polar regions. *Whitton BA, Potts M [eds] The ecology of cyanobacteria Kluwer, Dordrecht***:** 321-340.

Vincent W, Quesada A. (2012). Cyanobacteria in high latitude lakes, rivers and seas. *Whitton, B. A [eds].* Ecology of Cyanobacteria II: Their Diversity in Space and Time, Springer, New York: 371-385

Wada H, Murata N. (1990). Temperature-induced changes in the fatty-acid composition of the cyanobacterium, *Synechocystis* PCC6803. *Plant Physiol* **92:** 1062-1069.

Wilson A, Ajlani G, Verbavatz JM, Vass I, Kerfeld CA, Kirilovsky D. (2006). A soluble carotenoid protein involved in phycobilisome-related energy dissipation in cyanobacteria. *Plant Cell* **18:** 992-1007.

Wood AM, Phinney DA, Yentsch CS. (1998). Water column transparency and the distribution of spectrally distinct forms of phycoerythrin- containing organisms. *Mar Ecol Prog Ser* **162:** 25-31.

Zinser ER, Johnson ZI, Allison C, Karaca E, Veneziano D, Chisholm SW. (2007). Influence of light and temperature on *Prochlorococcus* ecotype distributions in the Atlantic Ocean. *Limnol Oceanogr* **52:** 2205-2220.

Zwirglmaier K, Heywood JL, Chamberlain K, Woodward EM, Zubkov MV, Scanlan DJ. (2007). Basin-scale distribution patterns of picocyanobacterial lineages in the Atlantic Ocean. *Environ Microbiol* **9:** 1278-1290.

Zwirglmaier K, Jardillier L, Ostrowski M, Mazard S, Garczarek L, Vaulot D *et al.* (2008). Global phylogeography of marine *Synechococcus* and *Prochlorococcus* reveals a distinct partitioning of lineages among oceanic biomes. *Environ Microbiol* **10:** 147-161.

Legends to Figures

Figure 1: Location of isolation sites of the six marine *Synechococcus* spp. used in this study.

Figure 2: Variations of relative cell density (cell mL^{-1}) expressed as % of initial cell density at the start of the experiment (**A**) and phycoerythrin to phycocyanin fluorescence emission ratio (**B)** in the tropical (triangles), mid-latitude (squares) and high latitude (circles) marine *Synechococcus* strains during six days of cold stress ($n \geq 4$).

Figure 3: Variations of state transition amplitude as measured by non photochemical quenching of fluorescence associated to state transition (NPQ_{ST}; **A**) and photosystem II quantum yield (F_V/F_M; **B**) in the tropical (triangles), mid-latitude (squares) and high latitude (circles) marine *Synechococcus* strains during six days of cold stress ($n \geq 4$).

Figure 4: Relative variations of the β-subunit of phycoerythrins I and II (A) and of the D1 protein (B) estimated by immunoreactions in tropical, mid-latitude and high latitude marine *Synechococcus* strains during five days of cold stress.

Figure 5: Variations of the β-carotene to chl *a* ratio (g/g) in the tropical (triangles), mid-latitude (squares) and high latitude (circles) marine *Synechococcus* strains during six days of cold stress ($n \geq 4$).

Figure 6: Growth rate as a function of temperature in the tropical (triangles), mid-latitude (squares) and high latitude (circles) marine *Synechococcus* strains. Error bars are standard deviation from the mean based on 4 replicates ($n \geq 4$).

Figure 7: Maximum likelihood (ML) analysis of the *petB* gene (based on 559 aligned aminoacids) retrieved from 74 marine cultured isolates of *Synechococcus*. For each strain, sea surface temperatures at the isolation site are indicated according to the color scale. Numbers at nodes correspond to bootstrap values from ML, Posterior probability of Bayesian inference (BI; ranging between 0 and 1) and bootstraps for neighbor-joining (NJ) method. Bootstraps, represented as a percentage, were obtained through 1000 repetitions for each method, and only values higher than 70% are shown on the phylogenetic tree. Filled circles correspond to nodes supported by values higher than 70/0.8/80 for ML/BI/NJ methods, respectively. Empty circles correspond to nodes fully supported by the three methods. The six *Synechococcus* strains used in this study are in bold. *Synechococcus* sp. WH5701, affiliated to the subcluster 5.2, was used as an outgroup. The nomenclature described by Mazard et al. (2012a) was retained for the clade/ecotype numbers.

Titles and legends to tables

Table 1: Information regarding the *Synechococcus* strains used in this study. The pigment type nomenclature is described in Six *et al.* 2007c and Humily *et al.* in press.

1055

Strain name	A15-37	M16.1	WH7803	ROS8604	MVIR-16-2	MVIR-18-1
RCC #	2526	791	752	2380	1594	2385
Pigment type	3a	3a	3a	3a	3a	3a
Isolation site	Offshore Mauritania	Gulf of Mexico	Sargasso Sea	English Channel	Southern Norwegian Sea	Southern Norwegian Sea
Isolation latitude	23°33’ N	27°42’ N	33° 45’ N	48° 43’ N	60° 19’ N	61° 00’ N
Isolation longitude	19°59’ W	91°18’ W	67° 30’ W	3° 59’ W	3° 29’ W	1° 59’ E
Isolation date	29/09/2004	09/02/2004	03/07/1978	24/11/1986	21/07/2007	23/07/2007
Isolation Depth (m)	10	275	25	1	10	25
Isolation temperature (°C)	24.53	24.15	25.85	12.81	11.99	13.98

Table 2: Photophysiological features of the six marine *Synechococcus* strains, acclimated at 22°C under 80 µmol photons m^{-2} s^{-1}.

Strain	A15-37	M16.1	WH7803	ROS8604	MVIR-16-2	MVIR-18-1
Orange fluorescence	0.05 ± 0.01	0.18 ± 0.01	0.80 ± 0.06	1.10 ± 0.22	0.45 ± 0.04	0.21 ± 0.07
PE:PC	2.70 ± 0.10	3.50 ± 0.70	2.00 ± 0.20	2.70 ± 0.20	2.40 ± 0.10	2.00 ± 0.30
F_v:F_M	0.64 ± 0.03	0.57 ± 0.07	0.61 ± 0.07	0.53 ± 0.03	0.57 ± 0.01	0.60 ± 0.02
NPQ_{ST}	0.48 ± 0.04	0.20 ± 0.07	0.47 ± 0.09	0.36 ± 0.01	0.43 ± 0.02	0.50 ± 0.01
Chl *a* (fg cell^{-1})	2.21 ± 0.81	2.62 ± 0.81	17.5 ± 1.41	9.52 ± 1.61	2.75 ± 0.39	5.57 ± 0.26
Zeaxanthin (fg cell^{-1})	1.47 ± 0.54	2.06 ± 0.59	5.20 ± 0.62	6.54 ± 1.71	2.05 ± 0.25	3.05 ± 0.07
β-carotene (fg cell^{-1})	0.08 ± 0.01	0.15 ± 0.05	1.16 ± 0.16	0.88 ± 0.09	0.22 ± 0.02	0.40 ± 0.02
Zeaxanthin : Chl *a* (g/g)	0.67 ± 0.07	0.80 ± 0.06	0.30 ± 0.03	0.69 ± 0.08	0.75 ± 0.03	0.53 ± 0.04
β-carotene : Chl *a* (g/g)	0.059 ± 0.028	0.085 ± 0.010	0.070 ± 0.001	0.094 ± 0.018	0.081 ± 0.004	0.071 ± 0.02

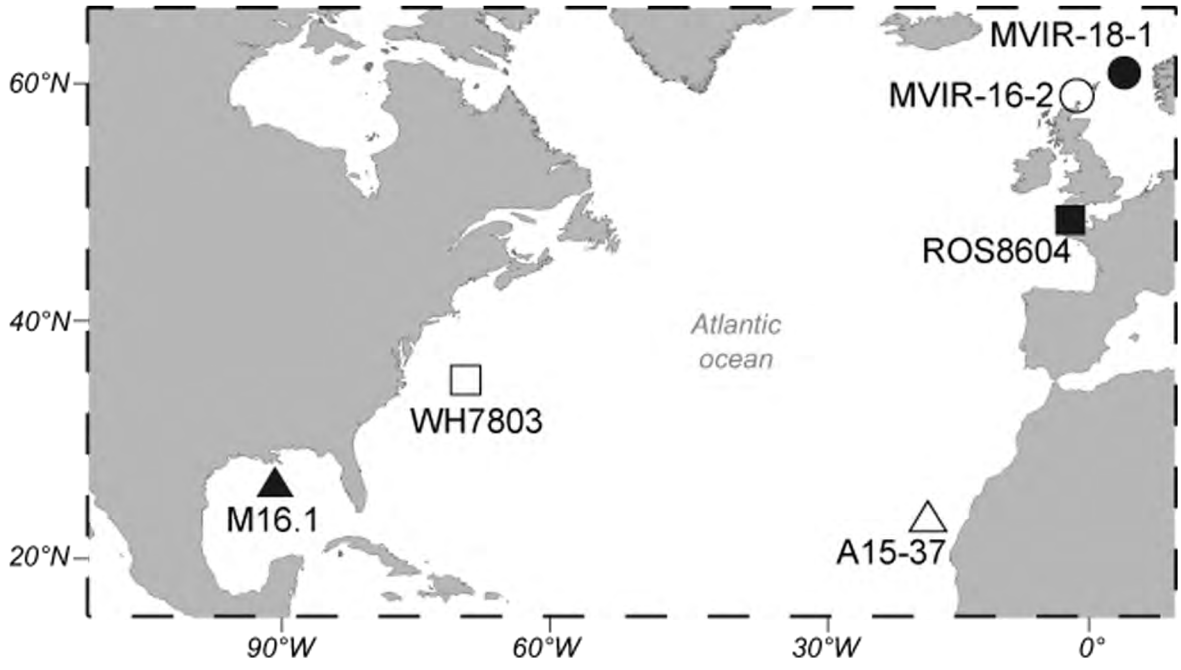
MVIR-18-1
MVIR-16-2
ROS8604
Atlantic
ocean
WH7803
M16.1
A15-37
60°N
40°N
20°N
90°W
60°W
30°W
0°

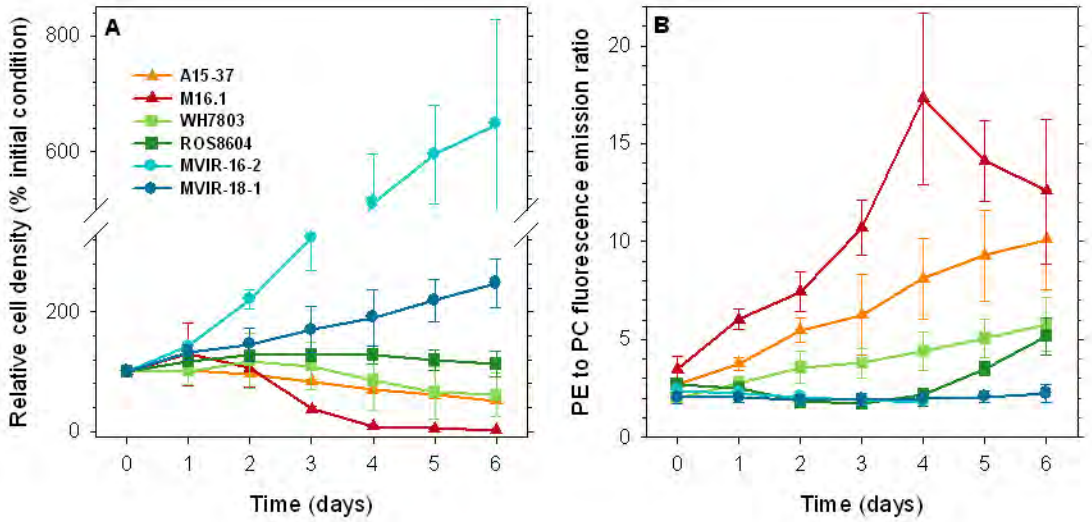
A
B
A15-37
M16.1
WH7803
ROS8604
MVIR-16-2
MVIR-18-1
Relative cell density (% initial condition)
PE to PC fluorescence emission ratio
Time (days)
Time (days)
0
200
600
800
5
10
15
20
0
1
2
3
4
5
6

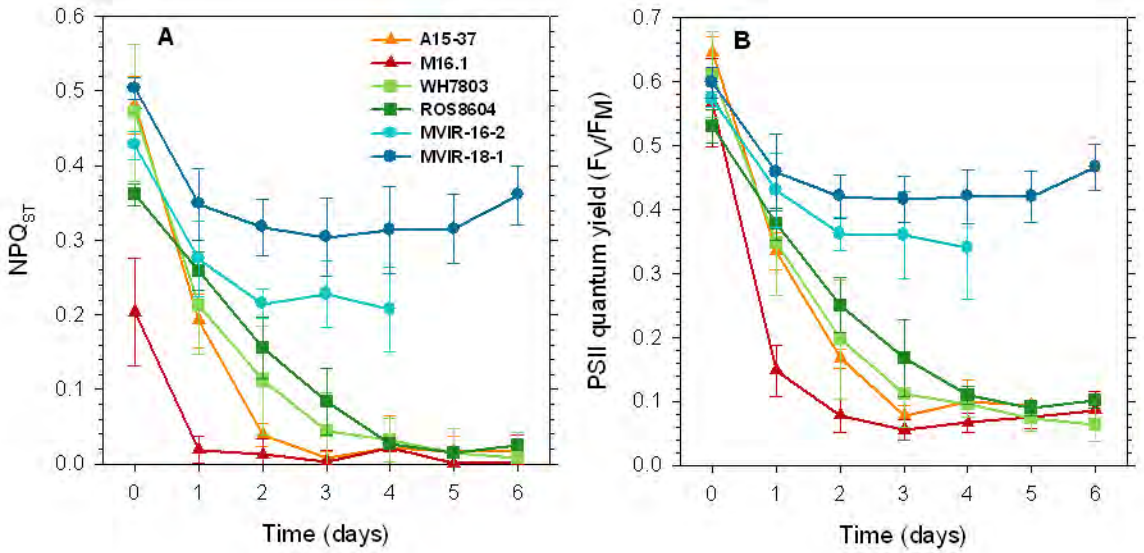
A
B
A15-37
M16.1
WH7803
ROS8604
MVIR-16-2
MVIR-18-1
NPQST
PSII quantum yield (FV/FM)
Time (days)
Time (days)
0.0
0.1
0.2
0.3
0.4
0.5
0.6
0.7
0
1
2
3
4
5
6

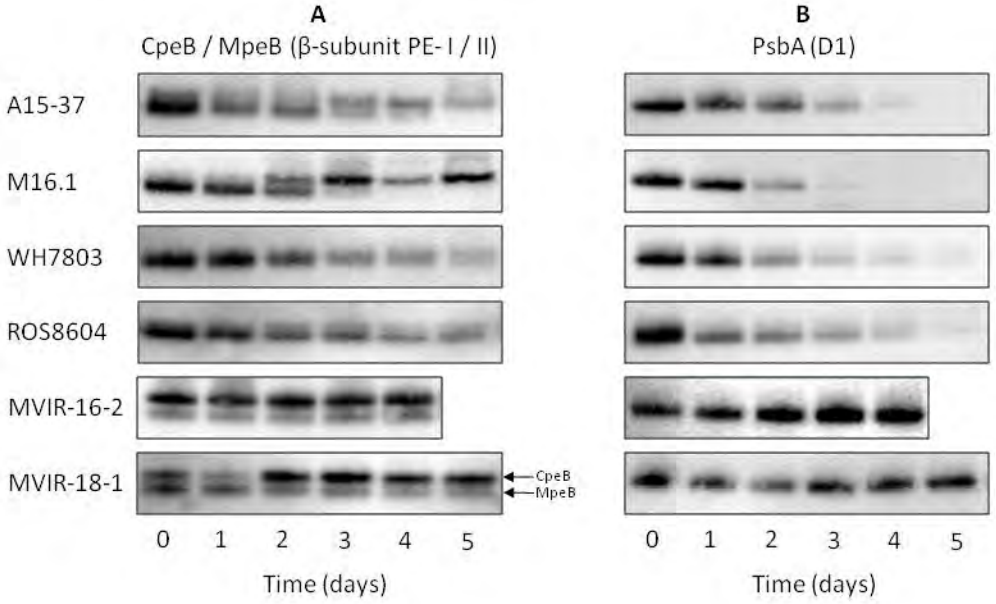
A
CpeB / MpeB (β-subunit PE- I / II)
B
PsbA (D1)
A15-37
M16.1
WH7803
ROS8604
MVIR-16-2
MVIR-18-1
CpeB
MpeB
0 1 2 3 4 5
Time (days)
0 1 2 3 4 5
Time (days)

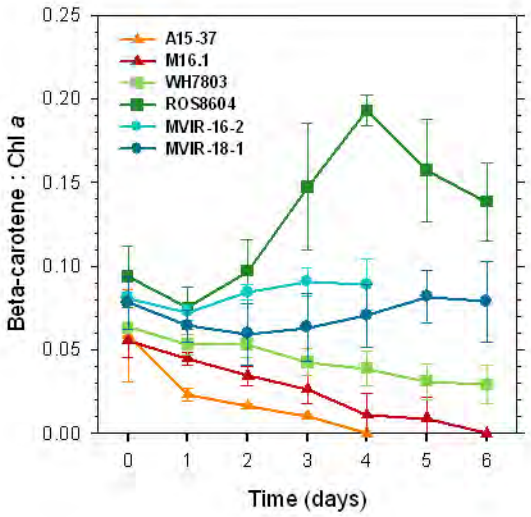
A15-37
M16.1
WH7803
ROS8604
MVIR-16-2
MVIR-18-1
Beta-carotene : Chl a
0.25
0.20
0.15
0.10
0.05
0.00
0
1
2
3
4
5
6
Time (days)

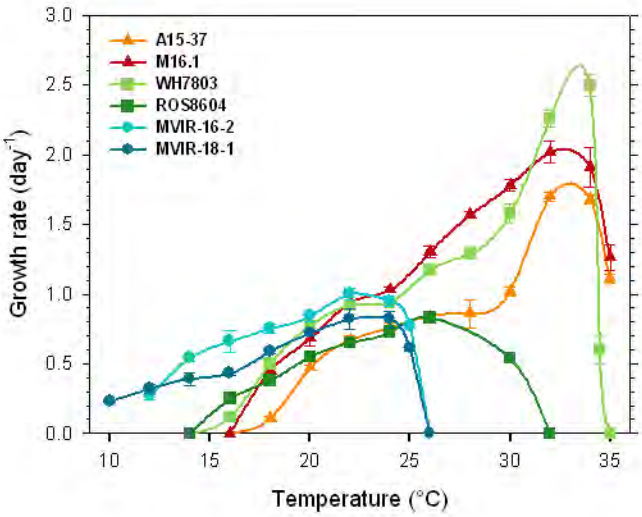
A15-37
M16.1
WH7803
ROS8604
MVIR-16-2
MVIR-18-1
Growth rate (day-1)
Temperature (°C)
0.0
0.5
1.0
1.5
2.0
2.5
3.0
10
15
20
25
30
35

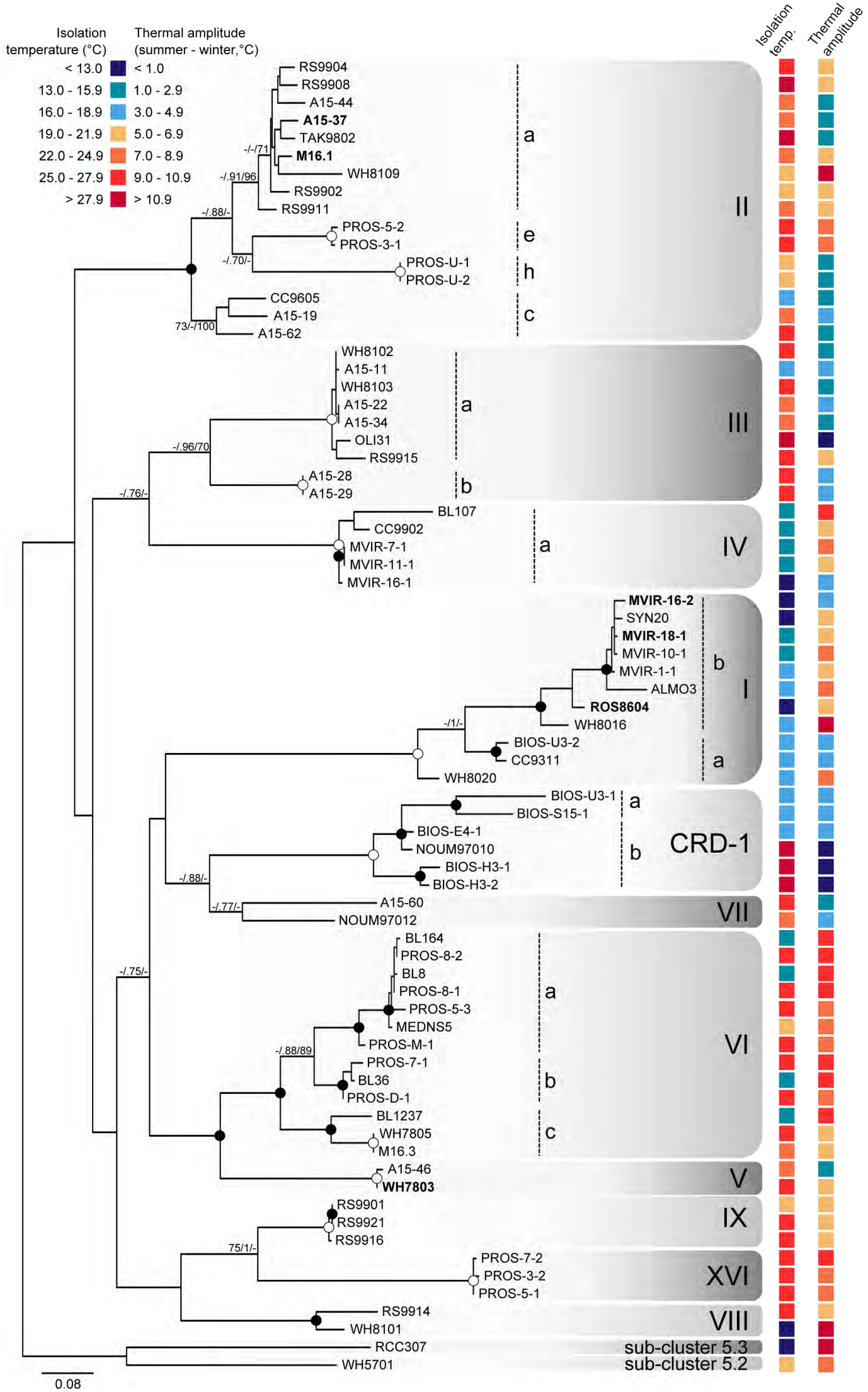
Isolation temperature (°C)
Thermal amplitude (summer - winter,°C)
< 13.0
13.0 - 15.9
16.0 - 18.9
19.0 - 21.9
22.0 - 24.9
25.0 - 27.9
> 27.9
< 1.0
1.0 - 2.9
3.0 - 4.9
5.0 - 6.9
7.0 - 8.9
9.0 - 10.9
> 10.9
Isolation temp.
Thermal amplitude
RS9904
RS9908
A15-44
A15-37
TAK9802
M16.1
WH8109
RS9902
RS9911
PROS-5-2
PROS-3-1
PROS-U-1
PROS-U-2
CC9605
A15-19
A15-62
-/-/71
-/.91/96
-/.88/-
-/.70/-
73/-/100
a
e
h
c
II
WH8102
A15-11
WH8103
A15-22
A15-34
OLI31
RS9915
A15-28
A15-29
-/.96/70
-/.76/-
a
b
III
BL107
CC9902
MVIR-7-1
MVIR-11-1
MVIR-16-1
a
IV
MVIR-16-2
SYN20
MVIR-18-1
MVIR-10-1
MVIR-1-1
ALMO3
ROS8604
WH8016
BIOS-U3-2
CC9311
WH8020
-/1/-
b
a
I
BIOS-U3-1
BIOS-S15-1
BIOS-E4-1
NOUM97010
BIOS-H3-1
BIOS-H3-2
-/.88/-
a
b
CRD-1
A15-60
NOUM97012
-/.77/-
VII
BL164
PROS-8-2
BL8
PROS-8-1
PROS-5-3
MEDNS5
PROS-M-1
PROS-7-1
BL36
PROS-D-1
BL1237
WH7805
M16.3
-/.75/-
-/.88/89
a
b
c
VI
A15-46
WH7803
V
RS9901
RS9921
RS9916
IX
PROS-7-2
PROS-3-2
PROS-5-1
75/1/-
XVI
RS9914
WH8101
VIII
RCC307
WH5701
sub-cluster 5.3
sub-cluster 5.2
0.08

Supplementary information

Supplementary tables

Table S1: Time (days) needed for recovery of initial values of photosynthetic parameters (photosystem II quantum yield, F_V/F_M; non photochemical quenching associated to state transitions, NPQ_{ST}; and phycoerythrin to phycocyanin fluorescence emission ratio, PE:PC) and to reach stationary phase at 22°C, after 6 days of cold stress at 13°C, for *Synechococcus* spp. M16.1, WH7803 and ROS8604. *Synechococcus* sp. A15-37 was not able to recover from cold stress when replaced under initial conditions.

Strain	F_V/F_M	NPQ_{ST}	PE:PC
M16.1	13.0 ± 1.4	14 ± 2.0	13.0 ± 1.7
WH7803	5.0 ± 1.8	5.5 ± 1.9	5.0 ± 0.8
ROS8604	5.7 ± 1.1	5.3 ± 0.6	4.3 ± 0.6

Table S2: Characteristics of marine *Synechococcus* strain isolation sites and accession numbers of the 74 *petB* sequences used in the phylogenetic study. Isolation temperatures were determined at the isolation site and date using satellite data and thermal amplitude was calculated using the average summer and winter temperature over 10 years (2002-2012; see methods).

Strain name	RCC number	Isolation latitude (°N)	Isolation longitude (°E)	Isolation ocean	Isolation region	Isolation date	Isolation depth (m)	Isolation temperature (°C)	Seawater thermal amplitude (°C)	*petB* Accession number
A15-11	2569	45.58	-18.23	North Atlantic	Eastern to the MAR [1]	06/06/1981	58	18.25	4.03	JF307472
A15-19	2525	38.53	-20.21	North Atlantic	Eastern to the MAR [1]	09/24/2004	75	22.02	4.48	JF307478
A15-22	1097	35.50	-20.51	North Atlantic	Northern gyre (edge)	09/25/2004	15	23.78	4.07	JF307480
A15-28	2556	31.15	-20.43	North Atlantic	Northern gyre (edge)	09/25/2004	10	25.15	3.08	JF307482
A15-29	2536	31.15	-20.43	North Atlantic	Northern gyre (edge)	09/26/2004	15	25.15	3.08	JF307483
A15-34	1101	29.70	-16.58	North Atlantic	Morocco upwelling	09/27/2004	40	24.61	2.50	JF307485
A15-37	2526	23.33	-19.59	North Atlantic	Morocco upwelling	09/29/2004	10	24.53	1.64	JF307486
A15-44	2527	21.41	-17.50	North Atlantic	Morocco upwelling	10/01/2004	20	22.61	2.09	KF443066
A15-46	2375	21.22	-18.49	North Atlantic	Morocco upwelling	09/30/2004	70	23.30	1.78	JF307490
A15-60	2554	17.37	-20.57	North Atlantic	Cabo Verde islands	10/04/2004	10	26.02	1.32	JF307495
A15-62	2374	17.37	-20.57	North Atlantic	Cabo Verde islands	10/04/2004	15	26.02	1.27	JF307497
ALMO3	2432	36.11	-1.51	Mediterranean sea	Alboran sea	05/01/1991	0	17.51	7.64	JF307500
BIOS-E4-1	2533	-33.60	-73.22	South Pacific	Chile upwelling	12/06/2004	40	16.56	3.32	JF307519
BIOS-H3-1	1018	-9.40	-136.59	South Pacific	Central HNLC area	11/02/2004	100	28.08	0.32	JF307514

BIOS-H3-2	1030	-9.40	-136.59	South Pacific	Central HNLC area	11/04/2004	30	28.08	0.32	JF307521
BIOS-S15-1	1023	-30.47	-95.26	South Pacific	Gyre	11/24/2004	100	18.66	4.07	JF307516
BIOS-U3-1	2534	-31.52	-91.25	South Pacific	Gyre	11/28/2004	40	16.56	3.32	JF307517
BIOS-U3-2	2532	-33.00	-73.20	South Pacific	Chile upwelling	12/08/2004	30	16.56	3.32	JF307511
BL107	515	41.43	3.33	Mediterranean sea	Balearic sea	03/15/2001	1800	13.89	9.00	AATZ00000000
BL1237	-	41.40	2.48	Mediterranean sea	Balearic sea	12/22/2000	-	15.25	9.45	JF307501
BL164	-	41.40	2.48	Mediterranean sea	Balearic sea	24/12/2000	3	15.25	9.45	JF307503
BL36	508	41.40	2.48	Mediterranean sea	Balearic sea	12/24/2000	0	15.25	9.45	JF307531
BL8		41.40	2.48	Mediterranean sea	Balearic sea	12/21/2000	-	15.25	9.45	JF307506
CC9311	1086	31.90	-124.16	North Pacific	California current	12/26/2000	95	16.59	2.29	CP000435
CC9605	753	30.41	-123.98	North pacific	California current	01/01/1993	-	18.02	2.03	CP000110
CC9902	2673	32.90	-117.25	North pacific	California current	10/01/1996	5	15.56	4.38	CP000097
M16.1	791	27.42	-91.18	North Altantic	Gulf of Mexico	02/09/2004	275	24.15	5.45	JF307548
M16.3	792	27.42	-91.18	North Altantic	Gulf of Mexico	02/09/2004	275	24.15	5.45	JF307549
MEDNS5	2368	41.00	6.00	Mediterranean sea	Balearic sea	07/01/1993	80	21.75	8.80	JF307539
MinSyn016	307	39.10	6.10	Mediterranean sea	Balearic sea	06/20/1996	15	21.08	8.80	CT978603
MVIR-16-1	2570	60.19	-3.29	North Atlantic	North sea	07/21/2007	10	11.99	3.06	KF443070
MVIR-16-2	3010	60.19	-3.29	North Atlantic	North sea	07/21/2007	10	11.99	3.06	KF443071
MVIR-7-1	1648	53.90	2.47	North Atlantic	North sea	07/10/2007	10	15.69	8.06	KF443073
MVIR-1-1	1708	48.46	-3.56	North Atlantic	North sea	07/04/2007	10	16.14	5.54	KF443067
MVIR-11-1	1695	56.56	3.59	North Atlantic	North sea	07/14/2007	10	15.09	5.24	KF443069
MVIR-10-1	1688	55.40	2.16	North Atlantic	North sea	07/13/2007	55	15.02	7.44	KF443068
MVIR-18-1	2385	61.00	1.59	North Atlantic	North sea	07/23/2007	25	13.98	6.01	KF443072

NOUM97010	66	0.00	-180.00	South pacific	Eastern HNLC area	11/04/1996	80	28.65	.70	JF307546
NOUM97012	67	-22.20	166.20	South pacific	New Caledonia coast	11/19/1996	70	24.42	3.31	JF307547
OLI31	44	-5.60	-150.00	South pacific	Central HNLC area	11/11/1994	70	28.56	0.33	JF307510
PROS-3-1	321	38.00	3.50	Mediterranean sea	Balearic sea	09/16/1999	5	25.79	8.84	JF307529
PROS-3-2	316	38.00	3.50	Mediterranean sea	Balearic sea	09/16/1999	110	25.79	8.84	JF307524
PROS-5-1	318	36.29	13.19	Mediterranean sea	Thyrrhenian sea	09/18/1999	65	26.41	8.32	JF307526
PROS-5-2	374	36.29	13.19	Mediterranean sea	Thyrrhenian sea	09/18/1999	25	26.41	8.32	JF307537
PROS-5-3	528	33.60	22.10	Mediterranean sea	Ionian sea	09/20/1999	50	26.59	7.36	JF307545
PROS-7-1	2381	37.24	15.37	Mediterranean sea	Thyrrhenian sea	09/26/1999	5	25.99	9.33	JF307531
PROS-7-2	317	37.24	15.37	Mediterranean sea	Thyrrhenian sea	09/26/1999	90	25.99	9.33	JF307525
PROS-8-1	527	39.70	14.50	Mediterranean sea	Thyrrhenian sea	09/27/1999	110	25.41	10.08	JF307544
PROS-8-2	523	39.70	14.50	Mediterranean sea	Thyrrhenian sea	09/27/1999	70	25.41	10.08	JF307541
PROS-D-1	319	43.24	7.49	Mediterranean sea	Gulf of lion	09/30/1999	15	23.72	8.81	JF307469
PROS-M-1	324	36.29	13.19	Mediterranean sea	Ionian sea	09/18/1999	5	26.41	8.32	JF307470
PROS-U-1	2369	30.80	-10.30	North Atlantic	Maroccan upwelling	09/12/1999	5	21.51	2.80	JF307538
PROS-U-2	442	30.80	-10.30	North Atlantic	Maroccan upwelling	09/12/1999	5	21.51	2.80	JF307540
ROS8604	2380	48.43	-3.59	North Atlantic	English Channel	11/24/1986	0	12.81	5.10	JF307527
RS9901	2529	29.28	34.55	Indian ocean	Red Sea	03/29/1999	1	21.07	5.64	JF307552
RS9902	2376	29.28	34.55	Indian ocean	Red Sea	03/23/1999	1	21.07	5.64	JF307553
RS9904	543	29.28	34.55	Indian ocean	Red Sea	06/14/1999	10	25.69	5.64	JF307554
RS9908	2530	31.28	34.55	Indian ocean	Red Sea	09/07/1999	-	28.37	5.64	JF307558
RS9911	550	29.28	34.55	Indian ocean	Red Sea	05/11/1999	10	23.77	5.64	JF307561
RS9914	553	29.28	34.55	Indian ocean	Red Sea	10/18/1999	10	26.98	5.64	JF307564

RS9915	2553	29.28	34.55	Indian ocean	Red Sea	10/18/1999	10	23.98	5.64	JF307565
RS9916	555	29.28	34.55	Indian ocean	Red Sea	11/22/1999	10	25.67	5.64	AAUA00000000
RS9921	559	29.28	34.55	Indian ocean	Red Sea	11/22/1999	150	25.67	5.64	JF307567
SYN20	2035	60.37	5.41	North Atlantic	North Sea	-	0	9.99 [2]	6.97	JF307568
TAK9802	2528	-14.30	-145.20	South Pacific	Takapoto atoll	02/06/1998	7	29.81	1.10	JF307523
WH5701	1084	41.05	-72.75	North Atlantic	Sargasso sea	01/01/1957	-	6.03	13.31	AANO00000000
WH7803	752	33.45	-67.30	North Atlantic	Sargasso sea	07/03/1978	25	25.85	5.88	CT971583
WH7805	1085	33.44	-67.30	North Altantic	Sargasso Sea	06/30/1978	-	25.85	5.88	AAOK00000000
WH8016	2535	41.53	-70.67	North Altantic	Sargasso Sea	06/01/1980	-	17.83	12.06	JF307569
WH8020	2437	38.41	-69.19	North Altantic	Sargasso Sea	06/16/1980	50	16.89	8.37	JF307571
WH8101	2555	41.53	-70.67	North Altantic	Sargasso Sea	01/01/1981	-	5.77	11.90	JF307572
WH8102	539	22.29	-65.36	North Altantic	Carribean Sea	03/15/1981	-	25.78	2.55	BX548020
WH8103	29	28.30	-67.23	North Altantic	Sargasso Sea	03/17/1981	-	25.45	2.90	JF307573
WH8109	2033	39.29	-70.28	North Altantic	Sargasso sea	06/01/1981	-	21.60	10.19	ACNY00000000

[1] MAR : Mid Atlantic Ridge

[2] Annual mean of sea surface temperature at the isolation site over the past 10 years (see methods).

Supplementary Figures

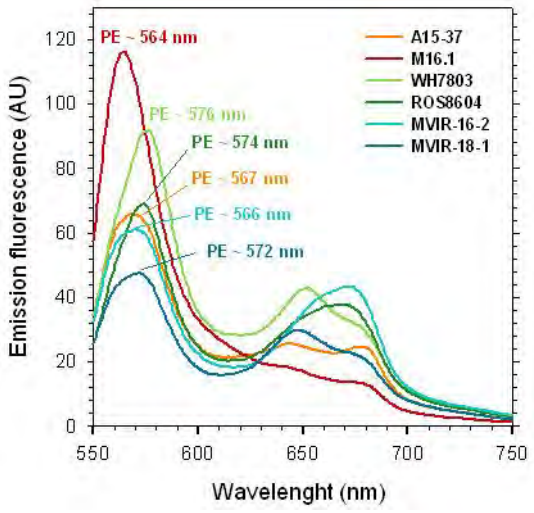

Figure S1: Fluorescence emission spectra (excitation at 530 nm) of the six *Synechococcus* strains used in this study. Wavelengths of phycoerythrin (PE) maxima are indicated on the figure, while phycocyanin emission maxima are 650, 644, 652, 655, 652 and 656 nm respectively for *Synechococcus* spp. A15-37, M16.1, WH7803, ROS8604, MVIR-16-2 and MVIR-18-1.

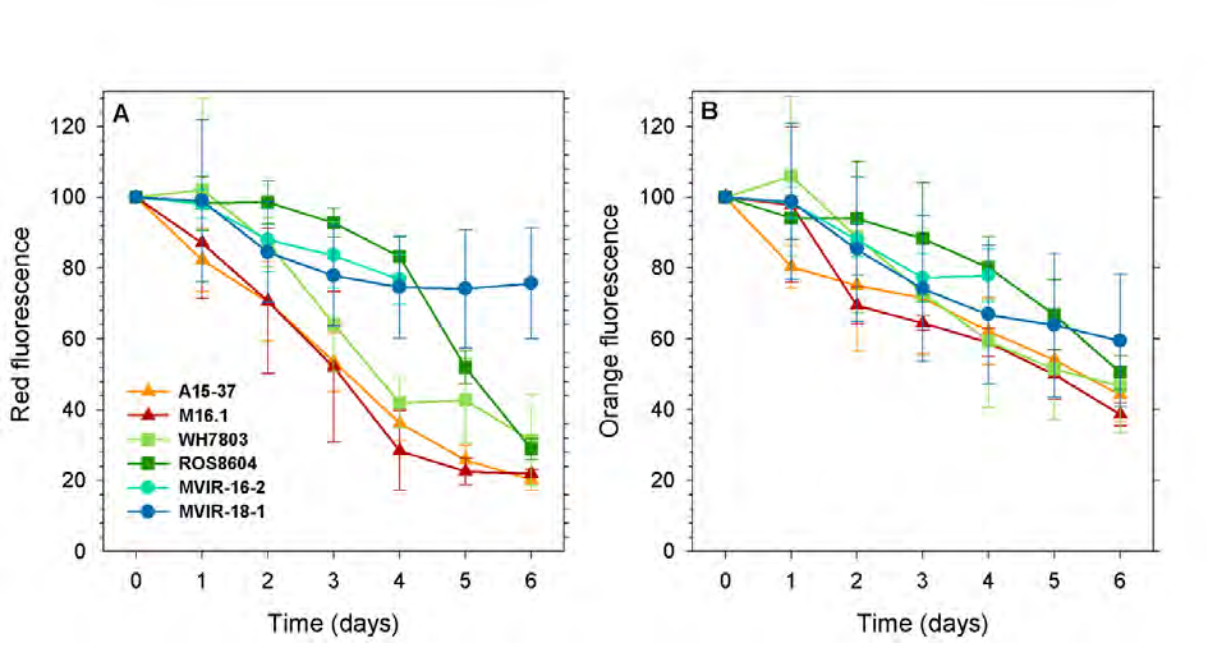

Figure S2: Variations of red (A) and orange (B) fluorescence in the tropical (triangles), mid-latitude (squares) and high latitude (circles) marine *Synechococcus* strains during six days of cold stress.